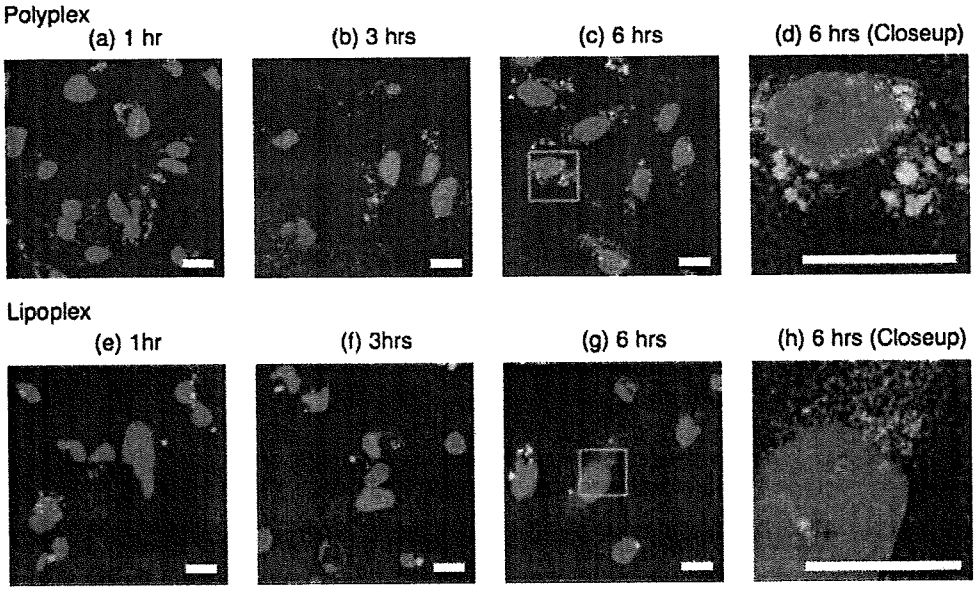

Figure 5. Confocal laser-scanning spectro-microscopy. Polyplex (a–d) and lipoplex (e–h) were administered to cells. Distribution and F/C ratio of double-labeled pDNA was analysed at 1(a,e), 3(b,f), and 6 (c,d,g,h) h after transfection. At 6 h after transfection, Keima-Red (yellow) fluorescence was detected in cells transfected with both polyplexes and lipoplexes. Pixels with F/C ratio ≥0.4 were colored green. Pixels with F/C ratios <0.4 were colored red. The nucleus was stained with Hoechst 33342 (blue). Close-up pictures (d,h) are shown of the green pixels identified in the nucleus at 6 h. Scale bar = 20 μm

cytoplasm and nucleus (Figure 5e). Most of the clumps were green.

At 3 h after transfection using polyplex, red clumps with a wide variation in size were observed in the cytoplasm and nucleus (Figure 5b). The number of green clumps was smaller than that observed at 1 h after transfection. Using lipoplex, large red clumps were observed in the cytoplasm, some adjoined to the nuclear membrane (Figure 5f). The number of green clumps was also smaller than that observed at 1 h after transfection.

At 6 h after transfection, the Keima-Red expression was detected with both transfection methods. Green pixels were present in the nucleus of Keima-Red positive cells (Figures 5c, 5d, 5g and 5h). Almost all cells challenged with polyplex had red clumps in the nucleus (Figure 5c), whereas, for the cells challenged with lipoplex, a fraction of cells lacked either green or red pixels in the nucleus (Figure 5 g). The close-up photographs depict green pixels in the nucleus of Keima-Red positive cells (Figures 5d and 5h).

Overall cell counts at 6 h after transfection

The cells were divided by the Keima-Red expression and then classified by the presence or absence of the green and/or red pixels in the nucleus (Table 1). After transfection using polyplex, 108 out of 110 cells (98.2%) had fluorescent clumps in the nucleus. Thirty-six of 44 Keima-Red positive cells (81.8%) contained green pixels in the nucleus. Thirteen of 66 Keima-Red negative cells (19.7%) had green pixels. Fifty-one of 66 Keima-Red negative cells (77.3%) had red pixels but no green pixels. After transfection using lipoplex, 13 of 16 Keima-Red positive cells (81.2%) had green pixels. Two of 53 Keima-Red negative cells (3.8%) had green pixels, whereas 38 of 53 Keima-Red negative cells (71.7%) had neither green nor red pixels.

Discussion

The present study aimed to understand how the conformational change of pDNA affects the gene expression. The double-labeling method of pDNA was used in our previous studies to observe the condensed state of pDNA inside the gene carriers. The advantage of using double-labeled pDNA is that it allows observation of the nanoscale

Table 1. Number of cells with intranuclear pixels

Intranuclear localization of green and red pixels	Keima-Red expression			
	Polyplex		Lipoplex	
	Positive	Negative	Positive	Negative
Green (+) /Red (+)	36 (81.8%)	13 (19.7%)	10 (62.5%)	2 (3.8%)
Green (+) /Red (−)	0	0	3 (18.8%)	0
Green (−) /Red (+)	8 (18.2%)	51 (77.3%)	2 (12.5%)	13 (24.5%)
Green (−) /Red (−)	0	2 (3.0%)	1 (6.3%)	38 (71.7%)
Subtotal	44	66	16	53
Total	110		69	

Overall cell counts at 6 h after transfection. The nuclei of the cells expressing or not expressing Keima-Red were optically sliced and explored for green and red pixels. Positive rates (44/110 or 16/69) do not represent credible transfection efficiencies because positive cells are nonrandomly selected and captured.

DOI: 10.1002/jgm

transition of pDNA in the physiological condition. This method can not only detect conformational transition from the decondensed to condensed state of pDNA, but also can also monitor the adverse transition from the condensed to decondensed state in a time scale manner [10,11]. Furthermore, the present study is superior to our previous studies for the several reasons. First, the covalent attachment of fluorophores retains the pDNA expression competency, to allow direct observation of both pDNA localization and expression. Keima-Red was chosen as a reporter gene because the Keima-Red protein has a large Stokes shift of maximal absorption at 440 nm and emission at 620 nm, which is beneficial for reducing the interference with the fluorophores of fluorescein and Cy3. Second, the observation was focused on the pDNA involved in the nucleus, but not in the entire cell, to selectively acquire the information from the site of transcription. Third, confocal microscopy has evolved into confocal laser-scanning spectromicroscopy. Consequently, from the spectra obtained from each pixel on the cell images, we were able to perform linear unmixing before the F/C ratio calculation to reduce background noise.

Polyplex and lipoplex are two distinct and representative nonviral carrier systems [3,13]. Although both systems form complexes through electrostatic interactions, cationic polymers typically condense the pDNA more efficiently than cationic lipids. The changes in the emission spectrum (Figures 1a and 1b) indicate that FRET between fluorescein and Cy3 was triggered by the condensation of pDNA inside the pDNA/LPEI complexes (polyplex). Spectral analysis revealed that complexation with LipofectAMINE 2000 reagent induced little change in the emission spectrum compared to free pDNA (Figure 1a). This may be a result of dilution of the cationic lipospermine in DOPE and a relatively large N/P, both allowing DNA to be sandwiched in between lipid multilayers without experiencing closest DNA/DNA contacts [14]. Fluctuation of the spectra was observed in a variety of fluorescent clumps obtained from cell images, suggesting a change in the pDNA condensation state through intracellular processes (Figures 1b and 1c).

The transition of pDNA from condensed to decondensed conformation was evaluated in 10 mM Tris-HCl solution by adding poly(aspartic acid) solution into the polyplex (Figure 2). The polyanions such as poly(aspartic acid) induce an exchange reaction with pDNA, facilitating pDNA decondensation and liberation from the polyplexes [10,11,15]. The exchange reaction dynamics showed a S-shaped curve consisting of lag, exponential, gradual, and saturation phases. The lag phase where the F/C ratios were maintained below 0.4 indicates a condensed state of pDNA. The number of donor–acceptor pairs undergoing FRET (i.e. the number of donor–acceptor pairs within the Forster distance in each pDNA molecule) maintained the maximum value. The exponential phase indicates that the addition of poly(aspartic acid) over the critical unit molar ratio triggered the conformational change of pDNA. As pDNA decondensation proceeded, the number of donor–acceptor pairs with a distance shorter than the Forster distance decreased, resulting in the increase in the F/C ratio. In this regard, F/C = 0.4 was defined as the critical ratio exerting the pDNA to take the fully condensed state. The saturation phase showed that the excessive addition of poly(aspartic acid) liberated pDNA to the F/C ratio of 2.5, but did not reach 2.8, which derived from free pDNA.

The frequency histogram of the F/C ratio showed a common F/C value of 0.4 for discriminating the Keima-Red positive and negative cells in both polyplex and lipoplex (Figure 4). Because the gene expression utilizes the innate transcription machinery in the cells, it is reasonable to assume that polyplex and lipoplex shared an identical cut-off value of pDNA decondensation to detect the gene expression. The histogram also shows that the F/C ratios fall within the range 0–1.0. According to the results of the experiment performed in 10 mM Tris-HCl (pH 7.4) solution, the pDNA with $0.4 < F/C < 1.0$ corresponds to the transient state from fully condensed to decondensed conformation (Figure 2). This result indicates that Keima-Red expression occurred even when the pDNA molecule was not in the fully decondensed state. Indeed, a recent study demonstrated that transcriptional factor has the ability to bind DNA with loosely condensed conformation [9]. Furthermore, it was shown, by evaluating transfection efficiency via nucleus microinjection [6] or *in vitro* cellular transcription assays [8], that the transcriptional competence of the polyplexes (PEI) was not impaired compared to that of free DNA.

To visualize the change of the F/C ratios in the cell images, the pixels were discriminated from each other based on the F/C ratio. Pixels with F/C ratios ≥ 0.4 were declared 'decondensed' pixels and colored green. Pixels with F/C ratios <0.4 were declared 'condensed' pixels and colored red. The intracellular processes of both polyplex and lipoplex were observed at 1, 3, and 6 h after transfection (Figure 5).

In polyplex, both green pixels and red pixels were widely observed inside the cells at 1 h after transfection. These green pixels can be interpreted as a fraction of pDNA in the process of decondensation. At 3 h after transfection, the number of green clumps was smaller than that observed at 1 h after transfection (Figure 5b), presumably because the polyplex that had been decondensed in the early stage of transfection might have been exocytosed, or disrupted in the endosome. At 6 h after transfection, green pixels were observed in the nucleus of Keima-Red positive cells (Figures 5c and 5d), consistent with the assumption that pDNA condensation may be related to the transgene expression.

In lipoplex, green clumps were observed in most of the cells, with a negligible portion of red clumps at 1 h after transfection (Figure 5e). This is consistent with the results of the fluorospectrometry (Figure 1a), which revealed that the pDNA is loosely packed in the lipoplex. At 3 h after transfection, large red clumps were observed in the cytoplasm, some adjoined to the nuclear membrane (Figure 5f). It is likely that loosely packed pDNA in

DOI: 10.1002/jgm

the lipoplex may undergo further condensation in the cytoplasm in a time-dependent manner. Otherwise, this may be due to the partial dilution of the carrier lipids into endosomal membranes, which brings DNA strands into closer contact. Detailed studies are needed to confirm this assumption. Similarly as in the case of polyplex, at 6 h after transfection, green pixels appeared in the nucleus of Keima-Red positive cells (Figures 5g and 5h).

The overall cell counts at 6 h after transfection revealed that more green pixels are observed in Keima-Red positive cells (Table 1). The majority of Keima-Red positive cells contained green pixels in the nucleus in both polyplex (81.8%) and lipoplex (81.2%). Thus, it is strongly suggested that the condensation state of pDNA had a close relationship to transgene expression, regardless of the transfection methods. By contrast, the composition of the Keima-Red negative cells was different between polyplex and lipoplex. In polyplex, the majority (77.3%) of Keima-Red negative cells were Green (−)/Red (+) in the nucleus. By contrast, in lipoplex, the majority (71.7%) of Keima-Red negative cells were Green (−)/Red (−) in the nucleus. These results indicate that the limiting factors for transgene expression in polyplex and lipoplex are different. Polyplex entry into the nucleus was observed in most of the cells, but an appreciable fraction of pDNA was still in the condensed state (red pixels), indicating that the pDNA decondensation in the nucleus appears to be the major limiting step for the transgene expression. Alternatively, the nuclear entry appeared to be the limiting factor for lipoplex transfection. This is consistent with the results of the histogram analysis shown in Figure 4, which demonstrates that, irrespective of the F/C ratio (x-axis), the counts on the y-axis in total are higher for polyplex than lipoplex, indicating that polyplex showed a higher nuclear import in total than lipoplex. Indeed, polyplex has more transgene efficiency than lipoplex at early hours when cells had no chance to divide [16]. Few Keima-Red positive cells were Green (−) in the nucleus. A possible explanation for this result is that those nuclei might not have been scanned thoroughly by five confocal slices, leaving the bottom or the top unscanned. Another possibility is that those fluorescence of the pDNA were below the detection limit.

No proper method is available to clarify the relationship of pDNA decondensation inside the nucleus with transgene expression. We developed, for the first time, a method for directly imaging the decondensation process of pDNA in the nucleus with a close correlation to reporter gene expression. The pDNA decondensation in the nucleus, visualized by the spectral change via FRET of doubly-labeled pDNA, was revealed as the crucial factor determining the transgene expression in both polyplex and lipoplex. This approach will contribute to the development of effective gene carriers by illuminating the intracellular mechanisms regulating the DNA structure and gene expression.

As in endogenous DNA expression, the exogenous pDNA utilizes the innate transcription machinery in the nucleus to express the encoded protein. The disintegration of pDNA from polyplexes or lipoplexes, and the subsequent partial decondensation, should play a crucial role in facilitating transcription in the nucleus. From the standpoint of developing nonviral carriers with high efficacy of transcription, we also need to consider the processed condensation of pDNA required to both tolerate the cytoplasmic barriers and safely reach into the nucleus. In this regard, a balance between the stability required during trafficking and the facile decondensation in the nucleus is key to developing effective gene carriers, in either configuration of polyplexes or lipoplexes.

Acknowledgements

We specially thank Dr F. Ishidate (Carl Zeiss, Tokyo, Japan) for providing technical advice and support for the confocal laser-scanning spectromicroscopy. We also appreciate the technical assistance of Ms Y. Hasegawa. This work was supported by Core Research Program for Evolutional Science and Technology (CREST) from the Japan Science and Technology Corporation (JST) and Grants-in-Aid for Scientific Research from the Japanese Ministry of Education, Culture, Sports, Science and Technology (17390412).

References

1. Wolff JA. The 'grand' problem of synthetic delivery. *Nat Biotechnol* 2002; **20**: 768–769.
2. Lungwitz U, Breunig M, Blunk T, *et al.* Polyethylenimine-based non-viral gene delivery systems. *Eur J Pharm Biopharm* 2005; **60**: 247–266.
3. Elouahabi A, Ruysschaert JM. Formation and intracellular trafficking of lipoplexes and polyplexes. *Mol Ther* 2005; **11**: 336–347.
4. Zabner J, Fasbender AJ, Moninger T, *et al.* Cellular and molecular barriers to gene transfer by a cationic lipid. *J Biol Chem* 1995; **270**: 18997–19007.
5. Cornelis S, Vandenbranden M, Ruysschaert JM, *et al.* Role of intracellular cationic liposome-DNA complex dissociation in transfection mediated by cationic lipids. *DNA Cell Biol* 2002; **21**: 91–97.
6. Pollard H, Remy JS, Loussouarn G, *et al.* Polyethylenimine but not cationic lipids promotes transgene delivery to the nucleus in mammalian cells. *J Biol Chem* 1998; **273**: 7507–7511.
7. Schaffer DV, Fidelman NA, Dan N, *et al.* Vector unpacking as a potential barrier for receptor-mediated polyplex gene delivery. *Biotechnol Bioeng* 2000; **67**: 598–606.
8. Bieber T, Meissner W, Kostin S, *et al.* Intracellular route and transcriptional competence of polyethylenimine-DNA complexes. *J Control Release* 2002; **82**: 441–454.
9. Honore I, Grosse S, Frison N, *et al.* Transcription of plasmid DNA: influence of plasmid DNA/polyethylenimine complex formation. *J Control Release* 2005; **107**: 537–546.
10. Itaka K, Harada A, Nakamura K, *et al.* Evaluation by fluorescence resonance energy transfer of the stability of nonviral gene delivery vectors under physiological conditions. *Biomacromolecules* 2002; **3**: 841–845.
11. Itaka K, Harada A, Yamasaki Y, *et al.* In situ single cell observation by fluorescence resonance energy transfer reveals fast intra-cytoplasmic delivery and easy release of plasmid DNA complexed with linear polyethylenimine. *J Gene Med* 2004; **6**: 76–84.
12. Slattum PS, Loomis AG, Machnik KJ, *et al.* Efficient in vitro and in vivo expression of covalently modified plasmid DNA. *Mol Ther* 2003; **8**: 255–263.
13. Khalil IA, Kogure K, Akita H, *et al.* Uptake pathways and subsequent intracellular trafficking in nonviral gene delivery. *Pharmacol Rev* 2006; **58**: 32–45.

14. Ewert K, Evans HM, Ahmad A, *et al.* Lipoplex structures and their distinct cellular pathways. *Adv Genet* 2005; **53**: 119–155.
15. Katayose S, Kataoka K. Remarkable increase in nuclease resistance of plasmid DNA through supramolecular assembly with poly(ethylene glycol)-poly(L-lysine) block copolymer. *J Pharm Sci* 1998; **87**: 160–163.
16. Brunner S, Furtbauer E, Sauer T, *et al.* Overcoming the nuclear barrier: cell cycle independent nonviral gene transfer with linear polyethylenimine or electroporation. *Mol Ther* 2002; **5**: 80–86.

Intratracheal Gene Transfer of Adrenomedullin Using Polyplex Nanomicelles Attenuates Monocrotaline-induced Pulmonary Hypertension in Rats

Mariko Harada-Shiba[1], Itaru Takamisawa[1], Kanjiro Miyata[2,3], Takehiko Ishii[2,3], Nobuhiro Nishiyama[3,4], Keiji Itaka[3,4], Kenji Kangawa[5], Fumiki Yoshihara[6], Yujiro Asada[7], Kinta Hatakeyama[7], Noriya Nagaya[8] and Kazunori Kataoka[3,4,9]

[1]Department of Bioscience, National Cardiovascular Center Research Institute, Suita, Japan; [2]Department of Bioengineering, Graduate School of Engineering, The University of Tokyo, Tokyo, Japan; [3]Center for NanoBio Integration, The University of Tokyo, Tokyo, Japan; [4]Division of Clinical Biotechnology; Center for Disease Biology and Integrative Medicine, Graduate School of Medicine, The University of Tokyo, Tokyo, Japan; [5]National Cardiovascular Center Research Institute, Suita, Japan; [6]Division of Hypertension and Nephrology, National Cardiovascular Center, Suita, Japan; [7]Department of Pathology, Faculty of Medicine, University of Miyazaki, Miyazaki, Japan; [8]Department of Regenerative Medicine, National Cardiovascular Center Research Institute, Suita, Japan; [9]Department of Materials Engineering, Graduate School of Engineering, The University of Tokyo, Tokyo, Japan

Pulmonary arterial hypertension (PAH) is a life-threatening disease characterized by progressive PAH and right ventricular failure. Despite recent advances in therapeutic approaches using prostanoids, endothelin antagonists, and so on, PAH remains a challenging condition. To develop a novel therapeutic approach, we have established a nonviral gene delivery system of poly(ethylene glycol) (PEG)-based block catiomers, which form a polyplex nanomicelle with a nanoscaled core–shell structure in the presence of DNA. The polyplex nanomicelle from PEG-*b*-poly{*N*-[*N*-(2-aminoethyl)-2-aminoethyl]aspartamide} (PEG-*b*-P[Asp(DET)]), having ethylenediamine units at the side chain, showed ~100-fold increase in luciferase transgene expression activity in mouse lung via intratracheal administration with a minimal toxicity compared with the polyplex from linear poly(ethylenimine) (LPEI). The transfection activity was highest on day 3 after administration and remained detectable until day 14. PEG-*b*-P[Asp(DET)] polyplex nanomicelles were formulated with a therapeutic plasmid bearing the human adrenomedullin (*AM*) gene and intratracheally administered to rats with monocrotaline-induced pulmonary hypertension. The right ventricular pressure significantly decreased 3 days after administration as confirmed by a notable increase of pulmonary human AM mRNA levels. Intratracheal administration of PEG-*b*-P[Asp-(DET)] polyplex nanomicelles showed remarkable therapeutic efficacy with PAH animal models without compromising biocompatibility.

Received 29 July 2008; accepted 9 March 2009; published online 31 March 2009. doi:10.1038/mt.2009.63

INTRODUCTION

Idiopathic pulmonary arterial hypertension (PAH) is a rare disease characterized by a progressive increase in pulmonary vascular resistance, leading to right heart failure and death.[1] Recent advances in therapeutic approaches to PAH show promising targeting pathways believed to play critical pathogenic or pathophysiologic roles;[2] however, despite these findings, PAH remains a challenging condition.[3]

Adrenomedullin (AM), a peptide isolated from human pheochromocytoma,[4] has multiple beneficial effects on cardiovascular tissues, including a powerful hypotensive effect.[5] Moreover, AM is indicated for PAH because of its prodilatory effects and the abundance of AM receptors in the lung.[6] Inhalation of AM was reported to ameliorate PAH in animal models[7] as well as in PAH patients without inducing systemic hypotension, but this effect was transient.[8] To overcome these barriers, a new, efficacious, and long-lasting AM therapy for PAH is warranted.

Gene therapy is one of the strategic approaches to continuously supply therapeutic peptides or proteins to target tissues.[6] Gene delivery to the lung via inhalation can avoid many problems associated with intravenous delivery, such as immediate nuclease degradation in the blood stream and the difficulty associated with penetrating endothelial barriers. In this regard, AM-based gene therapy through intratracheal route for PAH may have a promise.[7] Successful gene delivery via inhalation strongly depends on the development of advanced gene vectors to protect the therapeutic plasmid, provide site-specific targeting, and effectively release these plasmids for the desired pharmacological effect.

To develop a novel gene therapy system, we utilized our established polymeric library consisting of poly(ethylene glycol) (PEG)-based block catiomers, which form core–shell polyplex nanomicelles with core sequestration of the therapeutic plasmid.[9,10]

Correspondence: Mariko Harada-Shiba, Department of Bioscience, National Cardiovascular Center Research Institute, 5-7-1 Fujishirodai, Suita, Osaka 565-8565, Japan. E-mail: mshiba@ri.ncvc.go.jp

These polyplex nanomicelles are well dispersed even in aqueous media containing serum proteins and protect plasmid DNA from degradation by nuclease *in vivo*.[11–13] We recently developed P[Asp(DET)], a poly(aspartamide) derivative bearing an *N*-(2-aminoethyl)aminoethyl group as the side chain, that showed improved transfection efficiency and biocompatibility compared to linear poly(ethylenimine) (LPEI).[14] The PEG-based block catiomer with P[Asp(DET)] was applied *in vivo* to deliver therapeutic plasmids for a murine, skull bone defect model and a rabbit carotid artery with neointima model; its successful therapeutic efficacy with these mammalian studies provided the impetus for expanded application into the treatment of intractable diseases suited for gene therapy.[15,16]

In this paper, we report advanced, pulmonary transfection efficiencies using intratracheally inhaled PEG-*b*-P[Asp(DET)] polymeric nanomicelles without compromising biocompatibility. The intratracheal administration of the *AM* gene by PEG-*b*-P[Asp-(DET)] polyplex nanomicelles reduced right ventricular pressure in PAH animal models without inducing inflammation, suggesting its suitability as a vector for translational research.

RESULTS

Reporter gene transfer using PEG-*b*-P[Asp(DET)] via intratracheal administration

Plasmids bearing the luciferase reporter gene were formulated with PEG-*b*-P[Asp(DET)] (N/P = 80) and LPEI (N/P = 6) and were sprayed intratracheally into ICR mice. Here, N/P ratio refers to the unit molar ratio of the amino group in the polymer to the phosphate group in the plasmid DNA. After 1 day, the mice were killed and the pulmonary tissues were harvested to quantify luciferase activity. PEG-*b*-P[Asp(DET)] polyplex nanomicelles showed nearly a 100-fold increase in luciferase levels than the LPEI controls (Figure 1). Figure 2 shows the time-dependent changes of luciferase gene expression in the pulmonary tissue with PEG-*b*-P[Asp(DET)] polyplex nanomicelles. Luciferase activity was highest on day 3, and remained detectable until day 14. To elucidate the effect of PEG-*b*-P([Asp(DET)]/pLuc N/P ratios on luciferase gene expression, a series of the nanomicelles formulated under the varying N/P ratios (20, 40, and 80) were also examined. Figure 3 shows an ~50-fold increase in luciferase expression from N/P = 20 to N/P = 80 over a 3-day period. Next, PEG-*b*-P[Asp(DET)] polyplex nanomicelles loaded with plasmid DNA bearing the yellow fluorescence protein (YFP) gene (N/P = 80) or LPEI/pYFP polyplexes (N/P = 6) were sprayed intratracheally in ICR mice. After 1 day, the pulmonary tissue was harvested and the YFP gene expression was visualized by fluorescence microscopy (Figure 4). Significantly higher fluorescence intensity was clearly seen in the lungs treated with the PEG-*b*-P[Asp(DET)] polyplex nanomicelle than the LPEI polyplexes; moreover, YFP fluorescence activity was distinctly visible for the animals treated with PEG-*b*-P[Asp(DET)] polyplex micelles in the secondary bronchi and lower pulmonary generations. To evaluate the toxicity, immunohistochemistry was conducted on the lung tissues after the transfection of LPEI/pLuc controls (N/P = 6) (Figure 5a–c) or PEG-*b*-P[Asp(DET)]/pLuc (N/P = 80) (Figure 5d–f). The lung administered with LPEI/pLuc showed moderate infiltration of neutrophils at the

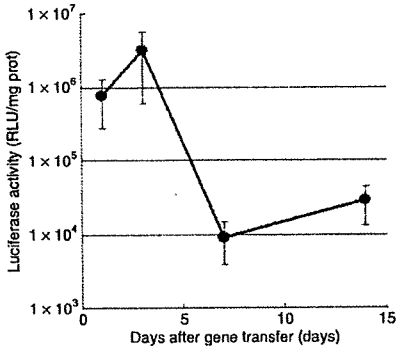

Figure 2 Time-dependent changes in gene expression after intratracheal administration of PEG-*b*-P[Asp(DET)] polyplex nanomicelle loaded with luciferase gene. The mice (five mice per group) were anesthetized and the polyplex nanomicelle was administered intratracheally. After the indicated time, the lung tissues were harvested, homogenized, and measured for luciferase activity (mean ± SEM, *N* = 5). PEG-*b*-P[Asp(DET)], PEG-*b*-poly{*N*-[*N*-(2-aminoethyl)-2-aminoethyl]aspartamide}.

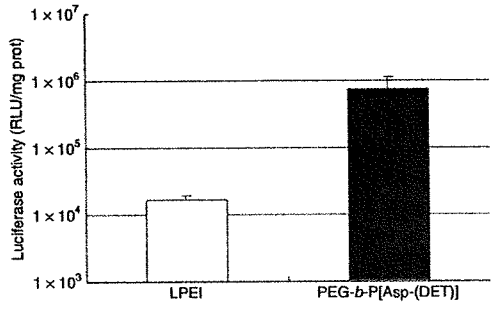

Figure 1 Luciferase gene expression by intratracheal administration of LPEI polyplex (N/P = 6) or PEG-*b*-P[Asp(DET)] polyplex nanomicelle (N/P = 80). Samples of the polyplex and the polyplex nanomicelle were prepared before the administration and left for 1 day. The mice (five mice per group) were anesthetized and the polyplex or the polyplex nanomicelle was administered intratracheally. At 24 hour postadministration, the lung tissues were harvested, homogenized, and measured for luciferase activity (mean ± SEM, *N* = 5). LPEI, linear poly(ethylenimine); PEG-*b*-P[Asp(DET)], PEG-*b*-poly{*N*-[*N*-(2-aminoethyl)-2-aminoethyl]aspartamide}.

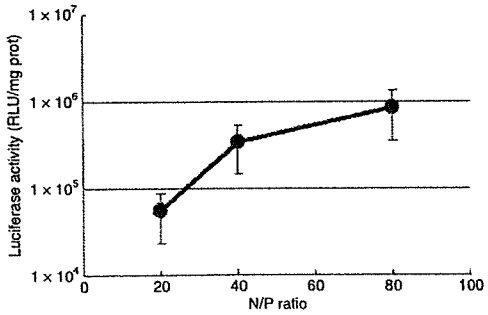

Figure 3 Charge-ratio-dependent changes in gene expression after intratracheal administration of the PEG-*b*-P[Asp(DET)] polyplex nanomicelle loaded with luciferase gene. The mice (five mice per group) were anesthetized and the polyplex nanomicelle was administered intratracheally. At 3 days postadministration, the lung tissues were harvested, homogenized, and measured for luciferase activity (mean ± SEM, *N* = 5). PEG-*b*-P[Asp(DET)], PEG-*b*-poly{*N*-[*N*-(2-aminoethyl)-2-aminoethyl]aspartamide}.

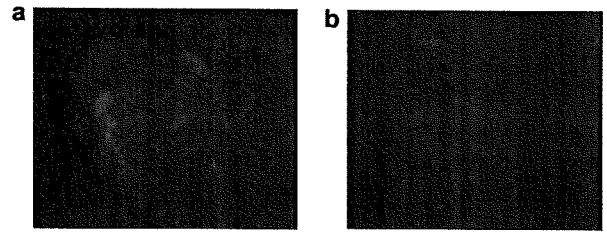

Figure 4 Fluorescence photographs of lungs transfected by intratracheal administration of YFP gene using PEG-*b*-P[Asp(DET)] polyplex nanomicelle or LPEI polyplex. (**a**) PEG-*b*-P[Asp(DET)] polyplex nanomicelle (N/P = 80), (**b**) LPEI polyplex (N/P = 6). The lung specimens were observed under a fluorescence microscope (SZX12; Olympus). LPEI, linear poly(ethylenimine); PEG-*b*-P[Asp(DET)], PEG-*b*-poly{*N*-[*N*-(2-aminoethyl)-2-aminoethyl]aspartamide}.

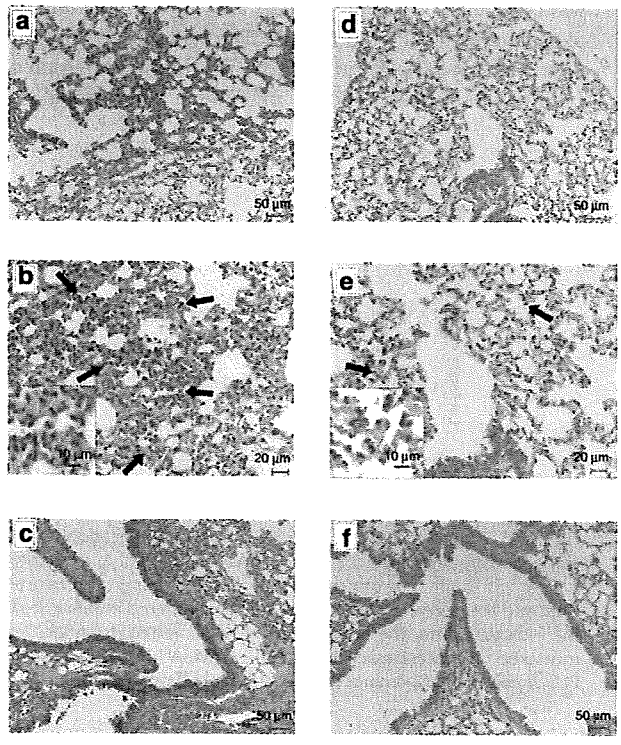

Figure 5 Representative photomicrographs of lung tissues 7 days postintratracheal administration of LPEI/pLuc (N/P = 6) (a–c) or PEG-*b*-P[Asp(DET)]/pLuc (N/P = 80) (d–f). The terminal bronchiole and alveoli of the lungs administered with LPEI polyplex (**a**,**b**) and PEG-*b*-P[Asp(DET)] polyplex nanomicelle (**d**,**e**) are shown. The neutrophil infiltration is indicated with arrows in the photomicrographs with higher magnification (**b**,**e**). Each inset is the picture with higher magnification. The bronchus of the lungs administered with LPEI polyplex (**c**) and PEG-*b*-P[Asp(DET)] polyplex nanomicelle (**f**) are also shown. LPEI, linear poly(ethylenimine); PEG-*b*-P[Asp(DET)], PEG-*b*-poly{*N*-[*N*-(2-aminoethyl)-2-aminoethyl]aspartamide}.

terminal bronchiole and alveoli as indicated (Figure 5a,b). However, the lung administered with PEG-*b*-P[Asp(DET)]/pLuc, neutrophilic infiltration was scattered and minimal or absent (Figure 5d,e). No apparent inflammatory infiltrate was observed in the bronchus of the both groups (Figure 5c,f). The findings thereby supported increased biocompatibility with the PEG-*b*-P[Asp(DET)] polyplex micelle. To further evaluate the toxicity of the gene carrier systems, mRNA levels of inflammatory cytokines in the pulmonary tissue were measured using real-time reverse transcriptase (RT)-PCR. A nontreated cohort was used as a control. Proinflammatory cytokine mRNA levels did not increase for intratracheally administered naked pLuc in saline or the PEG-*b*-P[Asp(DET)] polyplex micelles; however, LPEI/pLuc polyplexes revealed a twofold increase in TNF-α, interleukin (IL)-6, IL-10, and Cox-2 compared to the control (Figure 6a–d). Notably, PEG-*b*-P[Asp(DET)]/pLuc proinflammatory levels were statistically similar to the negative control cohorts in TNF-α, IL-6, IL-10, and Cox-2 mRNA levels.

Effect of *AM* gene transfer by PEG-*b*-P[Asp(DET)] polyplex nanomicelle in a rat model of PAH

After 4 weeks of monocrotaline injection, right ventricular pressure was increased to twice of the normal value (Figure 7). Notably, right ventricular pressure was decreased significantly by an intratracheal spray of the PEG-*b*-P[Asp(DET)] polyplex nanomicelle loaded with the expression vector of AM (N/P = 40). On the other hand, right ventricular pressure did not change significantly after administration of naked plasmid encoding the *AM* gene in saline or the LPEI polyplex loaded with the *AM* gene, or the polyplex nanomicelle loaded with the luciferase gene. The mRNA levels of human AM in the lung were measured by real-time RT-PCR (Figure 8). The lung transfected with the polyplex nanomicelle loaded with the expression vector of AM had high levels of AM mRNA. Alternatively, the levels were much lower in the lung transfected with the LPEI polyplex loaded with the expression vector of AM. The lung transfected with the polyplex nanomicelle loaded with the luciferase gene or with the naked *AM* gene in saline showed no expression of human AM.

DISCUSSION

The large number of human diseases presenting poor prognoses and limited efficacy with current therapeutic regimens necessitates the advent of alternative approaches. PAH is such a disease without a highly efficacious therapeutic regimen.[17] PAH patients are currently treated with a variety of drugs including prostacyclin, prostacyclin analogues, calcium channel blockers, nitric-oxide inhalation, angiotensin-converting enzyme inhibitors, endothelin receptor antagonists, and phosphodiesterase type 5 inhibitors; in severe cases lung transplantation and subsequent immunosuppression are necessary.[17] However, promising alternative therapies for PAH have been recently reported. For example, Champion *et al.* reported that adenoviral gene transfer of endothelial nitric-oxide synthase to the lungs of endothelial nitric-oxide synthase knockout mice ameliorates the symptoms of PAH.[18] Champion *et al.* also reported that adenoviral gene transfer of calcium gene-related peptide attenuates the symptoms of PAH.[19] Nagaya *et al.* reported that transfection of human prostacyclin synthase using hemagglutinating virus of Japan–liposomes ameliorates monocrotaline-induced PAH.[20] However, in these attempts, viral or viral-related vectors were used for the delivery of therapeutic genes and these gene carriers have the potential for immunogenicity and inflammatory response. In diseases where a single dose can cure or provide palliative care, viral vectors may be suitable; however, PAH therapy requires repeated

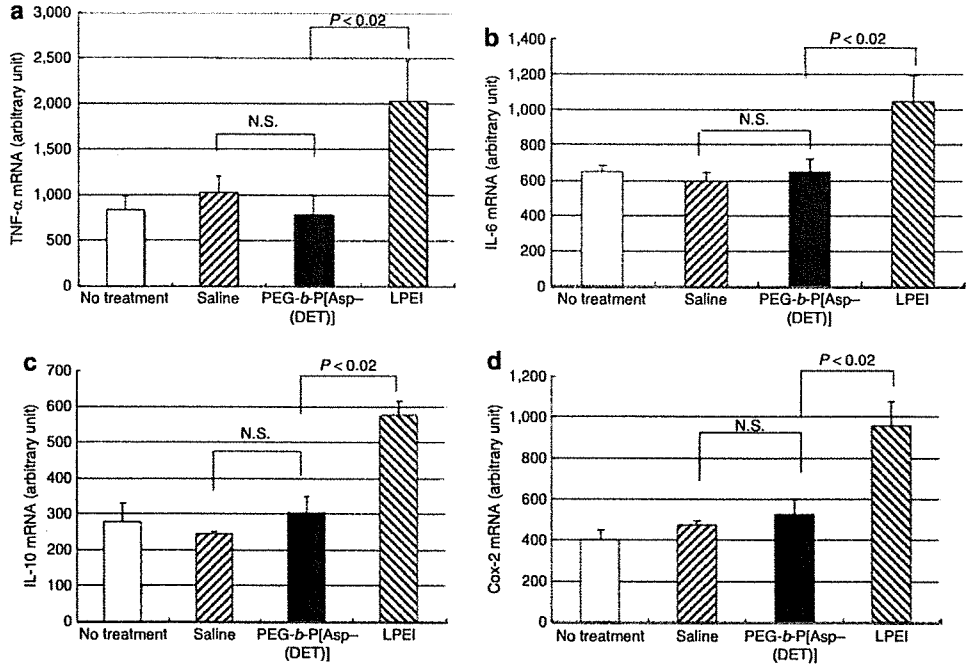

Figure 6 mRNA expression of inflammatory cytokines in lung tissues 7 days postintratracheal administration of luciferase gene in saline; LPEI polyplex with luciferase gene (N/P = 6); or PEG-*b*-P[Asp(DET)] polyplex nanomicelle with luciferase gene (N/P = 80) (mean ± SEM, $N = 4$). (**a**) TNF-α, (**b**) IL-6, (**c**) IL-10, (**d**) Cox-2. IL, interleukin; LPEI, linear poly(ethylenimine); TNF, tumor necrosis factor; PEG-*b*-P[Asp(DET)], PEG-*b*-poly{*N*-[*N*-(2-aminoethyl)-2-aminoethyl]aspartamide}.

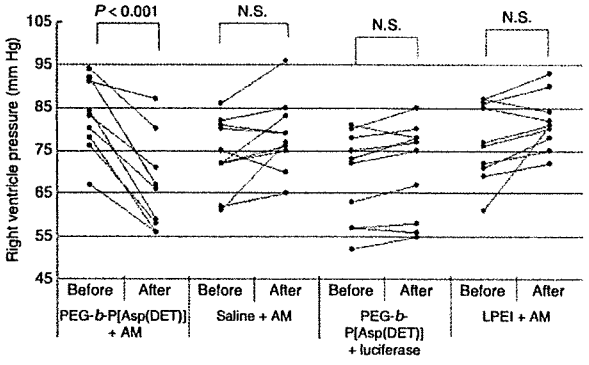

Figure 7 Effect of gene transfer on the right ventricle pressure in the PAH rat model. At 4 weeks after subcutaneous monocrotaline injection, a hemodynamic study was performed to measure the RV pressure indicated as "Before". The PEG-*b*-P[Asp(DET)] polyplex nanomicelle loaded with AM expression vector; AM expression vector in saline; PEG-*b*-P[Asp(DET)] polyplex micelle loaded with luciferase gene; or the LPEI polyplex loaded with AM expression vector were sprayed intratracheally. Three days later, a hemodynamic study was performed again to measure the RV pressure indicated as "After". AM, adrenomedullin; LPEI, linear poly(ethylenimine); PAH, pulmonary arterial hypertension; PEG-*b*-P[Asp(DET)], PEG-*b*-poly{*N*-[*N*-(2-aminoethyl)-2-aminoethyl]aspartamide}; RV, right ventricular.

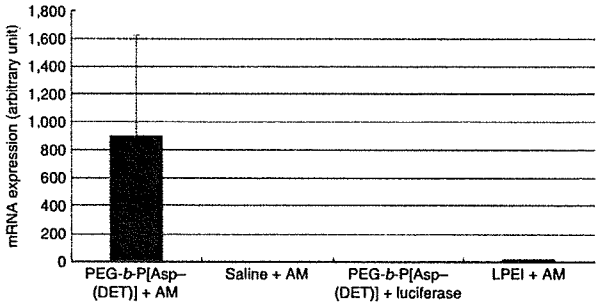

Figure 8 mRNA expression of human AM in the PAH rat model postintratracheal administration of PEG-*b*-P[Asp(DET)] polyplex nanomicelles loaded with the AM expression vector; AM expression vector in saline; PEG-*b*-P[Asp(DET)] polyplex nanomicelles loaded with the luciferase gene; or LPEI polyplexes loaded with the AM expression vector. Rats were transfected intratracheally at 4 weeks after subcutaneous monocrotaline injection. Three days later, lungs were harvested, homogenized, and measured for AM mRNA using real-time RT-PCR (mean ± SEM, $N = 4$). AM, adrenomedullin; LPEI, linear poly(ethylenimine); PAH, pulmonary arterial hypertension; PEG-*b*-P[Asp(DET)], PEG-*b*-poly{*N*-[*N*-(2-aminoethyl)-2-aminoethyl]aspartamide}.

administrations for efficacy, hence the utility of viral or viral-based gene therapy is contraindicated.

Alternatively, nonviral gene carriers have been recognized with several advantages over viral vectors in terms of safety, immunogenicity, and ease of manufacture. To develop a method of gene therapy suitable for clinical translation, four primary factors must be clearly addressed: (i) the gene carrier, (ii) the therapeutic gene, (iii) the route of administration, and (iv) patient compliance. In this study, we chose to further explore the promising (i) PEG-*b*-P[Asp(DET)] polyplex nanomicelle nonviral gene carrier system based upon our previous findings. Next, we chose (ii) *AM* as the therapeutic gene because of its reported effectiveness in the transient treatment of PAH. For the route of administration, we selected (iii) intratracheal administration to avoid the rapid propensity of nuclease degradation in the blood compartment and also that we might exploit the lung, based upon its enormous surface area, for

use as a therapeutic bioreactor for AM production. Pulmonary administration is a promising therapeutic route of administration in the clinic for its (iv) high patient compliance with utilization of an inhaler or nebulizer.

Recently, we have demonstrated that PEG-*b*-P[Asp(DET)] polyplex nanomicelles achieved amplified *in vitro* and *in vivo* transfection activity with minimal cytotoxicity.[14–16,21] With regard to the transfection mechanism, P[Asp(DET)] possesses the ethylenediamine side chain, which undergoes two-step protonation from the mono-protonated gauche form at physiological pH to di-protonated anti form at acidic pH, thereby exhibiting an effective buffering function in the acidic endosomal compartment.[22] Also, we revealed the membrane destabilization effect of P[Asp(DET)] responding to acidic endosomal pH conditions by hemolysis, leakage of cytoplasmic enzyme (lactate dehydrogenase assay), and confocal laser scanning microscopic observation.[22] Consequently, we observed the facilitated transport of Cy5-labeled plasmid DNA by the P[Asp(DET)] polyplexes from endo/lysosomal compartment into cytoplasm directly under the confocal laser scanning microscope in single cellular level.[22] Therefore, the increased transgene expression in Figure 3 may be a result of the facilitated translocation of the polyplex nanomicelles from the endosome to the cytoplasm based on the buffering capacity (proton sponge effect) and/or endosomal membrane-destabilizing effect of P[Asp(DET)] segment. The reason why a relatively high N/P ratio was required for the efficient transfection (Figure 3) may be because the membrane-destabilizing effect of P[Asp(DET)] is dependent on the polymer concentration as previously reported. Nevertheless, the PEG-*b*-P[Asp(DET)] polyplex nanomicelles displayed minimal cytotoxicity even at a high N/P ratio, which may be due to the pH-sensitive properties of P[Asp(DET)] segment.[22] The highly transfectable but less cytotoxic properties of PEG-*b*-P[Asp(DET)] polyplex nanomicelles motivated us to apply them to the gene therapy of PAH animal models through the intratracheal administration in this study.

A number of nonviral vectors including polyplex and lipoplex have been applied for *in vivo* intratracheal transfection. Special notice for the pulmonary gene delivery via airways is that the lung has the features critically influencing the transfection efficiency, such as the presence of surfactant, alveolar macrophages, and mucocilliary clearance mechanisms. In the early 1990s, lipoplex was used by aerosol delivery or intratracheal instillation. However, cationic lipids were shown to have a decreased transfection efficiency due to the interaction with lung surfactant compared to cationic polymer like PEI.[23,24] To overcome the surfactant barriers, cationic emulsion was used and showed much higher transfection activity compared with lipoplexes, such as lipofectin, lipofectamine, and DMRIE/c.[25] However, even for the cationic emulsion, the luciferase activity was limited to 55 pg/mg protein, which is significantly lower than the value attained by the polyplex nanomicelles loaded with PEG-*b*-P[Asp(DET)] [3,000,000 relative light unit/mg protein (135 ng/mg protein)] as reported here. Polyplexes made from cationic polymer was reported to show higher transfection efficiency compared with cationic lipoplexes for pulmonary gene delivery via airways.[23,24] PEI or modified PEI has been shown to be one of the most effective agents for constructing gene delivery systems available today with high levels of pulmonary gene transfer by airways.[26,27] Intratracheal injection of polyplex loaded with 22 kd of LPEI (ExGen 500) showed up to 20,000–40,000 relative light unit/mg protein of luciferase activity in the lung by adjusting N/P ratio. Worth noting is that the nanomicelles achieved two orders of magnitude higher value in luciferase gene expression compared to the LPEI polyplex. Furthermore, no induction of cytokine responses is appealing for the nanomicelles over LPEI polyplex (Figure 6), which was reported to induce the activation of $CD8^+$ and $CD4^+$ T cells, and Fas ligand–mediated antigen-induced cell death.[28,29]

To ameliorate the symptoms of PAH in animal models, several genes have been identified including: endothelial nitric-oxide synthase, inducible nitric-oxide synthase, prostacyclin synthase, calcium gene-related peptide, vascular endothelial growth factor, and hepatocyte growth factor.[18–20,30–36] We used AM as a therapeutic gene because of its high potency and long-term effectiveness as a vasodilator in the pulmonary vascular bed.[37] The effect of pulmonary vasodilation is mediated by cyclic adenosine monophosphate–dependent and nitric oxide–dependent mechanisms.[38] PAH patients have elevated plasma AM concentrations, which increase in step with the disease's severity[39,40] often resulting in pulmonary hypotension. In previous studies, intravenous administration[41] and inhalation[8] of the AM peptide showed acute hemodynamic and hormonal efficacy in PAH patients. However, despite alternative routes of delivery, the small AM peptide was rapidly degraded *in vivo* displaying a poor pharmacokinetic profile with a temporal window of only 30–45 minutes. For the treatment of PAH, sustained effect of AM is required. In this report, the therapeutic indicator for successful nonviral AM delivery was a decrease in the right ventricular pressure. Indeed, for the polyplex nanomicelle/pAM formulation, the right ventricular pressure did decrease, but more importantly the persistence of *AM* gene expression continued within a therapeutic range for a minimum of 3 days. The results indicate that the therapeutic approach using the polyplex nanomicelle as a vector does not require chronic infusion or very frequent inhalation, which will make the therapy more clinically applicable.

In this study, we succeeded in delivering DNA to the lung via intratracheal administration using the polyplex nanomicelles, resulting in extremely improved transfection efficiency with concomitant high biocompatibility. More specifically, the lung transfected with the polyplex nanomicelle had much lower toxicity than that transfected with the LPEI polyplex, according to the histological findings and measurement of the mRNA levels of inflammatory cytokines (Figure 6a–d). We also developed an effective treatment for the PAH rat model by delivering the therapeutic *AM* gene with polyplex nanomicelles from PEG-*b*-P[Asp(DET)]. These results showed a significant increase in transfection efficiently *in vivo* with intratracheal administration. The PEG-*b*-P[Asp(DET)] polyplex nanomicelle delivery system clearly showed promising *in vivo* results of transgene and therapeutic AM expression, when coupled with the clear visual, localization of the polyplex nanomicelles in the pulmonary tissue and the lack of proinflammatory responses. We posit that the PEG-*b*-P[Asp(DET)] nonviral gene carrier clearly shows those characteristics requisite for novel and advanced therapeutic systems ideally suited for translational research.

MATERIALS AND METHODS

Materials. An expression vector for YFP (RIKEN, Tokyo, Japan) was amplified in competent HB101 *Escherichia coli* and purified by Plasmid Giga Kits (Qiagen, Hilden, Germany). An expression vector for luciferase with a CAG promoter was provided by RIKEN. An expression vector for human AM was constructed as follows. The *EcoRI*/*Xho*I fragment of the full-length human AM complementary DNA (cDNA)[42] was ligated into the *EcoRI*/*Xho*I site of pcDNA1 (Invitrogen, Carlsbad, CA). The restriction maps of expression vector for luciferase and human AM cDNA are listed in **Supplementary Figure S1a,b**, respectively. To confirm that pcDNA/AM encodes AM, pcDNA/AM was transfected into Chinese hamster ovary cells, and the medium and the cells were collected for the measurement of immunoreactive AM using an AM radioimmunoassay Shionogi (Cosmic, Tokyo, Japan).

Animals. Male ICR mice weighing 25–30 g were administered the reporter gene intratracheally. Male Wistar rats weighing 100–120 g were used to make a model of PAH. All protocols were performed in accordance with the guidelines of the Animal Care Ethics Committee of the National Cardiovascular Center Research Institute (Osaka, Japan).

Synthesis and characterization of PEG-b-P[Asp(DET)]. PEG-*b*-P[Asp(DET)] was prepared as previously described.[14] Briefly, PEG-poly(β-benzyl-L-aspartate) (PEG-PBLA) diblock copolymer was synthesized by the ring-opening polymerization of β-benzyl-L-aspartate *N*-carboxy-anhydride from the terminal primary amino group of α-methoxy-ω-amino PEG (M_w: 12,000; Nippon Oil and Fats, Tokyo, Japan). Gel-permeation chromatography confirmed that the copolymer was unimodal with a narrow molecular weight distribution (M_w/M_n: 1.23), and the number of benzyl-L-aspartate repeating units was calculated to be 68 by ^{1}H-NMR. The N-terminal amino group of PEG-PBLA was then acetylated using acetic anhydride in dichloromethane solution to obtain PEG-PBLA-Ac. The obtained polymer was dissolved in distilled *N,N*-dimethylformamide (Wako Pure Chemical Industries, Osaka, Japan) and reacted with diethylenetriamine (Tokyo Kasei Kogyo, Tokyo, Japan) for 24 hours at 40 °C in a dry argon atmosphere to undergo aminolysis of the benzyl side chain. After 24 hours, the solution was slowly dripped into a 10% acetic acid solution and dialyzed (Spectra/Por Membrane, 3,500 molecular weight cutoff; Spectrum Laboratories, Rancho Dominguez, CA) against 0.01 N HCl and subsequently against distilled water. The final solution was lyophilized to obtain PEG-*b*-P[Asp(DET)] as the hydrochloride salt form. ^{1}H-NMR confirmed the complete substitution of benzyl ester of the polymer with diethylenetriamine through the aminolysis reaction, as well as the chemical structure of the obtained PEG-*b*-P[Asp(DET)] block copolymer.

Preparation of polyplex nanomicelles. The PEG-*b*-P[Asp(DET)] block copolymer and plasmid DNA were separately dissolved in 10 mmol/l HEPES buffer (pH 7.4). Both solutions were mixed at the indicated nitrogen/phosphate ratios [=(total amines in cationic segment)/(phosphates in plasmid DNA)] and incubated overnight at room temperature to make PEG-*b*-P[Asp-(DET)] polyplex nanomicelle. LPEI (ExGen; Cosmo Bio, Tokyo, Japan) polyplexes were prepared by mixing plasmid DNA and LPEI according to the manufacturer's protocol.

In vivo *gene delivery by intratracheal administration.* ICR mice were anesthetized by intraperitoneal administration of pentobarbital (30 mg/kg) (Dainippon Sumitomo Pharma, Osaka, Japan). Tracheostomies were performed under sterile conditions for PEG-*b*-P[Asp-(DET)] polyplex nanomicelle or LPEI polyplex (10 μg of DNA for each mouse) in a 50 μl of solution administration by a microsprayer Model IA-1C (Penn Century, Philadelphia, PA). After the indicated time, the mice were killed by cervical dislocation and the pulmonary tissues harvested. To measure luciferase activity, the pulmonary tissues were homogenized in a lysis buffer using a polytron. The lysate was then centrifuged at 14,000*g* for 10 minutes at 4 °C, and 20 μl of the supernatant was analyzed for luciferase activity by a Luminous CT-9000D luminometer (Dia-Iatron, Tokyo, Japan), according to a previously described method.[43] Background of luciferase activity in the lung was measured from the lung of mice after administration of saline, which was <3% of the total activity of day 14. All the data of luciferase activity were obtained by subtraction of background data. To detect YFP expression, mice were killed by cervical dislocation and the lungs harvested. Frozen sections (5-μm thick) of the lung specimens were visualized by a fluorescence microscope (SZX12; Olympus, Tokyo, Japan). To examine the histological features of the lung tissue, the specimens were also fixed in 4% paraformaldehyde and embedded in paraffin. Sections (3-μm thick) were stained with hematoxylin.

Isolation of RNA and cDNA synthesis. Total RNA was extracted using the Trizol method (Gibco BRL Life Technologies, Breda, Netherlands) according to the protocol provided by the manufacturer. The RNA was dissolved in RNAse-free water and quantified by a spectrophotometer. The cDNA was synthesized using the High Capacity cDNA Reverse Transcription Kit (Applied Biosystems, Foster City, CA).

Real-time RT-PCR. mRNA expression levels of TNF-α, IL-6, IL-10, Cox-2 and human AM were measured by quantitative real-time RT-PCR based on TaqMan chemistry (Applied Biosystems) using an ABI PRISM 7700 sequence detector (Applied Biosystems). The reaction mixture contained 0.5 μl of 5 μmol/l probe (final concentration, 100 nmol/l); 1 μl of 10 μmol/l forward primer and 1 μl of 10 μmol/l reverse primer (400 nmol/l final concentration of each primer); 12.5 μl of TaqMan Universal Mastermix, 5 μl of diethyl pyrocarbonate–treated water, and 5 μl of a cDNA sample. Assay controls were performed in the same TaqMan plate with no-template controls to test for the contamination of any assay reagents. The thermocycling conditions were initiated at 50 °C for 2 minutes with an enzyme activation step of 95 °C for 10 minutes followed by 40 PCR cycles of denaturation at 95 °C for 15 seconds, and anneal/extension at 60 °C for 1 minute.

Hemodynamic studies. Hemodynamic studies were performed 4 weeks after gene transfer. Rats were anesthetized with intraperitoneal pentobarbital (30 mg/kg) and placed on a heating pad to maintain body temperature 37–38 °C throughout the study. Under sterile conditions, a polyethylene catheter (PE-50; BD Biosciences, San Jose, CA) was inserted through the right jugular vein into the right ventricle to measure right ventricular pressure by a hemodynamic transducer (PowerLab 8/30; ADInstruments, Colorado Springs, CO).

Evaluation of gene transfer effect in a PAH rat model. Monocrotaline (60 mg/kg) was subcutaneously injected into male Wistar rats and left for 4 weeks to make a model of PAH. After 4 weeks, a hemodynamic study was performed to introduce a catheter into the right ventricle through the right jugular vein. The PEG-*b*-P[Asp(DET)] polyplex nanomicelle loaded with the AM expression vector (200 μg of DNA for each rat) in a 200 μl of solution was sprayed intratracheally. Three days later, a hemodynamic study was performed again and the gene transfer effect was evaluated. Pulmonary tissue specimens were frozen to measure *AM* gene expression by real-time RT-PCR.

Statistical analysis. All data are expressed as means ± SEM unless otherwise indicated. Comparisons of parameters among four groups were made by one-way analysis of variance, followed by Scheffe's multiple-comparison test. Paired *t*-test was applied for the comparison of the values before and after the gene transfection (Figure 7).

SUPPLEMENTARY MATERIAL

Figure S1. The restriction maps of expression vector for luciferase and human adrenomedullin cDNA.

ACKNOWLEDGMENTS

This work was supported by the Core Research Program for Evolutional Science and Technology from the Japan Science and Technology

Corporation, by Grants-in-Aid for Scientific Research from the Japanese Ministry of Health, Labor, and Welfare (H19-Nano-012 and H20-Genomu-Ippan-008), by the Program for the Promotion of Fundamental Studies in Health Sciences of the National Institute of Biomedical Innovation of Japan, and by the Takeda Science Foundation. We thank Keiko Jinno, Shoko Obora, Hiroko Miyata, Moto Ohira, and Eri Abe and Mutsumi Goda (National Cardiovascular Center Research Institute) for their excellent technical assistance, including animal care. We also thank Hisayuki Matsuo and Hitonobu Tomoike for their helpful discussion and advice, Darin Y. Furgeson (University of Wisconsin–Madison) for proofreading of this manuscript.

REFERENCES

1. Rubin, LJ (2006). Pulmonary arterial hypertension. *Proc Am Thorac Soc* **3**: 111–115.
2. Badesch, DB, Abman, SH, Ahearn, GS, Barst, RJ, McCrory, DC, Simonneau, G *et al.* (2004). Medical therapy for pulmonary arterial hypertension: ACCP evidence-based clinical practice guidelines. *Chest* **126**(1 Suppl): 35S–62S.
3. D'Alonzo, GE, Barst, RJ, Ayres, SM, Bergofsky, EH, Brundage, BH, Detre, KM *et al.* (1991). Survival in patients with primary pulmonary hypertension. Results from a national prospective registry. *Ann Intern Med* **115**: 343–349.
4. Kitamura, K, Kangawa, K, Kawamoto, M, Ichiki, Y, Nakamura, S, Matsuo, H *et al.* (1993). Adrenomedullin: a novel hypotensive peptide isolated from human pheochromocytoma. *Biochem Biophys Res Commun* **192**: 553–560.
5. Kitamura, K, Kangawa, K and Eto, T (2002). Adrenomedullin and PAMP: discovery, structures, and cardiovascular functions. *Microsc Res Tech* **57**: 3–13.
6. Nagaya, N, Mori, H, Murakami, S, Kangawa, K and Kitamura, S (2005). Adrenomedullin: angiogenesis and gene therapy. *Am J Physiol Regul Integr Comp Physiol* **288**: R1432–R1437.
7. Nagaya, N, Okumura, H, Uematsu, M, Shimizu, W, Ono, F, Shirai, M *et al.* (2003). Repeated inhalation of adrenomedullin ameliorates pulmonary hypertension and survival in monocrotaline rats. *Am J Physiol Heart Circ Physiol* **285**: H2125–H2131.
8. Nagaya, N, Kyotani, S, Uematsu, M, Ueno, K, Oya, H, Nakanishi, N *et al.* (2004). Effects of adrenomedullin inhalation on hemodynamics and exercise capacity in patients with idiopathic pulmonary arterial hypertension. *Circulation* **109**: 351–356.
9. Katayose, S and Kataoka, K (1997). Water-soluble polyion complex associates of DNA and poly(ethylene glycol)-poly(L-lysine) block copolymer. *Bioconjug Chem* **8**: 702–707.
10. Kakizawa, Y and Kataoka, K (2002). Block copolymer micelles for delivery of gene and related compounds. *Adv Drug Deliv Rev* **54**: 203–222.
11. Katayose, S and Kataoka, K (1998). Remarkable increase in nuclease resistance of plasmid DNA through supramolecular assembly with poly(ethylene glycol)-poly(L-lysine) block copolymer. *J Pharm Sci* **87**: 160–163.
12. Itaka, K, Yamauchi, K, Harada, A, Nakamura, K, Kawaguchi, H and Kataoka, K (2003). Polyion complex micelles from plasmid DNA and poly(ethylene glycol)-poly(L-lysine) block copolymer as serum-tolerable polyplex system: physicochemical properties of micelles relevant to gene transfection efficiency. *Biomaterials* **24**: 4495–4506.
13. Harada-Shiba, M, Yamauchi, K, Harada, A, Takamisawa, I, Shimokado, K and Kataoka, K (2002). Polyion complex micelles as vectors in gene therapy—pharmacokinetics and *in vivo* gene transfer. *Gene Ther* **9**: 407–414.
14. Kanayama, N, Fukushima, S, Nishiyama, N, Itaka, K, Jang, WD, Miyata, K *et al.* (2006). A PEG-based biocompatible block catiomer with high buffering capacity for the construction of polyplex micelles showing efficient gene transfer toward primary cells. *ChemMedChem* **1**: 439–444.
15. Itaka, K, Ohba, S, Miyata, K, Kawaguchi, H, Nakamura, K, Takato, T *et al.* (2007). Bone regeneration by regulated *in vivo* gene transfer using biocompatible polyplex nanomicelles. *Mol Ther* **15**: 1655–1662.
16. Akagi, D, Oba, M, Koyama, H, Nishiyama, N, Fukushima, S, Miyata, T *et al.* (2007). Biocompatible micellar nanovectors achieve efficient gene transfer to vascular lesions without cytotoxicity and thrombus formation. *Gene Ther* **14**: 1029–1038.
17. Nossaman, BD, Gur, S and Kadowitz, PJ (2007). Gene and stem cell therapy in the treatment of erectile dysfunction and pulmonary hypertension; potential treatments for the common problem of endothelial dysfunction. *Curr Gene Ther* **7**: 131–153.
18. Champion, HC, Bivalacqua, TJ, Greenberg, SS, Giles, TD, Hyman, AL, Kadowitz, PJ (2002). Adenoviral gene transfer of endothelial nitric-oxide synthase (eNOS) partially restores normal pulmonary arterial pressure in eNOS-deficient mice. *Proc Natl Acad Sci USA* **99**: 13248–13253.
19. Champion, HC, Bivalacqua, TJ, Toyoda, K, Heistad, DD, Hyman, AL and Kadowitz, PJ (2000). *In vivo* gene transfer of prepro-calcitonin gene-related peptide to the lung attenuates chronic hypoxia-induced pulmonary hypertension in the mouse. *Circulation* **101**: 923–930.
20. Nagaya, N, Yokoyama, C, Kyotani, S, Shimonishi, M, Morishita, R, Uematsu, M *et al.* (2000). Gene transfer of human prostacyclin synthase ameliorates monocrotaline-induced pulmonary hypertension in rats. *Circulation* **102**: 2005–2010.
21. Masago, K, Itaka, K, Nishiyama, N, Chung, UI and Kataoka, K (2007). Gene delivery with biocompatible cationic polymer: Pharmacogenomic analysis on cell bioactivity. *Biomaterials* **28**: 5169–5175.
22. Miyata, K, Oba, M, Nakanishi, M, Fukushima, S, Yamasaki, Y, Koyama, H *et al.* (2008). Polyplexes from poly(aspartamide) bearing 1,2-diaminoethane side chains induce pH-selective, endosomal membrane destabilization with amplified transfection and negligible cytotoxicity. *J Am Chem Soc* **130**: 16287–16294.
23. Bragonzi, A, Dina, G, Villa, A, Calori, G, Biffi, A, Bordignon, C *et al.* (2000). Biodistribution and transgene expression with nonviral cationic vector/DNA complexes in the lungs. *Gene Ther* **7**: 1753–1760.
24. Wiseman, JW, Goddard, CA, McLelland, D and Colledge, WH (2003). A comparison of linear and branched polyethylenimine (PEI) with DCChol/DOPE liposomes for gene delivery to epithelial cells *in vitro* and *in vivo*. *Gene Ther* **10**: 1654–1662.
25. Kim, TW, Chung, H, Kwon, IC, Sung, HC, Shin, BC and Jeong, SY (2005). Airway gene transfer using cationic emulsion as a mucosal gene carrier. *J Gene Med* **7**: 749–758.
26. Densmore, CL (2006). Advances in noninvasive pulmonary gene therapy. *Curr Drug Deliv* **3**: 55–63.
27. Furgeson, DY, Chan, WS, Yockman, JW and Kim, SW (2003). Modified linear polyethylenimine-cholesterol conjugates for DNA complexation. *Bioconjug Chem* **14**: 840–847.
28. Gautam, A, Densmore, CL and Waldrep, JC (2001). Pulmonary cytokine responses associated with PEI-DNA aerosol gene therapy. *Gene Ther* **8**: 254–257.
29. Regnstrom, K, Ragnarsson, EG, Koping-Hoggard, M, Torstensson, E, Nyblom, H and Artursson, P (2003). PEI—a potent, but not harmless, mucosal immuno-stimulator of mixed T-helper cell response and FasL-mediated cell death in mice. *Gene Ther* **10**: 1575–1583.
30. Budts, W, Pokreisz, P, Nong, Z, Van Pelt, N, Gillijns, H, Gerard, R *et al.* (2000). Aerosol gene transfer with inducible nitric oxide synthase reduces hypoxic pulmonary hypertension and pulmonary vascular remodeling in rats. *Circulation* **102**: 2880–2885.
31. Chicoine, LG, Tzeng, E, Bryan, R, Saenz, S, Paffett, ML, Jones, J *et al.* (2004). Intratracheal adenoviral-mediated delivery of iNOS decreases pulmonary vasoconstrictor responses in rats. *J Appl Physiol* **97**: 1814–1822.
32. Campbell, AI, Zhao, Y, Sandhu, R and Stewart, DJ (2001). Cell-based gene transfer of vascular endothelial growth factor attenuates monocrotaline-induced pulmonary hypertension. *Circulation* **104**: 2242–2248.
33. Gong, F, Tang, H, Lin, Y, Gu, W, Wang, W and Kang, M (2005). Gene transfer of vascular endothelial growth factor reduces bleomycin-induced pulmonary hypertension in immature rabbits. *Pediatr Int* **47**: 242–247.
34. Suhara, H, Sawa, Y, Fukushima, N, Kagisaki, K, Yokoyama, C, Tanabe, T *et al.* (2002). Gene transfer of human prostacyclin synthase into the liver is effective for the treatment of pulmonary hypertension in rats. *J Thorac Cardiovasc Surg* **123**: 855–861.
35. Ono, M, Sawa, Y, Fukushima, N, Suhara, H, Nakamura, T, Yokoyama, C *et al.* (2004). Gene transfer of hepatocyte growth factor with prostacyclin synthase in severe pulmonary hypertension of rats. *Eur J Cardiothorac Surg* **26**: 1092–1097.
36. Ono, M, Sawa, Y, Mizuno, S, Fukushima, N, Ichikawa, H, Bessho, K *et al.* (2004). Hepatocyte growth factor suppresses vascular medial hyperplasia and matrix accumulation in advanced pulmonary hypertension of rats. *Circulation* **110**: 2896–2902.
37. Lippton, H, Chang, JK, Hao, Q, Summer, W and Hyman, AL (1994). Adrenomedullin dilates the pulmonary vascular bed *in vivo*. *J Appl Physiol* **76**: 2154–2156.
38. Ishizaka, Y, Ishizaka, Y, Tanaka, M, Kitamura, K, Kangawa, K, Minamino, N *et al.* (1994). Adrenomedullin stimulates cyclic AMP formation in rat vascular smooth muscle cells. *Biochem Biophys Res Commun* **200**: 642–646.
39. Kakishita, M, Nishikimi, T, Okano, Y, Satoh, T, Kyotani, S, Nagaya, N *et al.* (1999). Increased plasma levels of adrenomedullin in patients with pulmonary hypertension. *Clin Sci (Lond)* **96**: 33–39.
40. Yoshibayashi, M, Kamiya, T, Kitamura, K, Saito, Y, Kangawa, K, Nishikimi, T *et al.* (1997). Plasma levels of adrenomedullin in primary and secondary pulmonary hypertension in patients <20 years of age. *Am J Cardiol* **79**: 1556–1558.
41. Nagaya, N, Nishikimi, T, Uematsu, M, Satoh, T, Oya, H, Kyotani, S *et al.* (2000). Haemodynamic and hormonal effects of adrenomedullin in patients with pulmonary hypertension. *Heart* **84**: 653–658.
42. Kitamura, K, Sakata, J, Kangawa, K, Kojima, M, Matsuo, H and Eto, T (1993). Cloning and characterization of cDNA encoding a precursor for human adrenomedullin. *Biochem Biophys Res Commun* **194**: 720–725.
43. de Wet, JR, Wood, KV, DeLuca, M, Helinski, DR and Subramani, S (1987). Firefly luciferase gene: structure and expression in mammalian cells. *Mol Cell Biol* **7**: 725–737.

GENE DELIVERY

ELSEVIER

Available online at www.sciencedirect.com

ScienceDirect

Journal of Controlled Release 122 (2007) 252–260

journal of controlled release

www.elsevier.com/locate/jconrel

PEG-based block catiomers possessing DNA anchoring and endosomal escaping functions to form polyplex micelles with improved stability and high transfection efficacy

Kanjiro Miyata [a,d], Shigeto Fukushima [b], Nobuhiro Nishiyama [c,d], Yuichi Yamasaki [b,d], Kazunori Kataoka [b,c,d,*]

[a] Department of Bioengineering, School of Engineering, The University of Tokyo, 7-3-1 Hongo, Bunkyo-ku, Tokyo 113-8656, Japan
[b] Department of Materials Engineering, School of Engineering, The University of Tokyo, 7-3-1 Hongo, Bunkyo-ku, Tokyo 113-8656, Japan
[c] Center for Disease Biology and Integrative Medicine, School of Medicine, The University of Tokyo, 7-3-1 Hongo, Bunkyo-ku, Tokyo 113-0033, Japan
[d] Center for NanoBio Integration, The University of Tokyo, 7-3-1 Hongo, Bunkyo-ku, Tokyo 113-8656, Japan

Received 26 May 2007; accepted 19 June 2007
Available online 27 June 2007

Abstract

For the development of polyplex systems showing a high transfection efficacy without a large excess of polycations, a lysine (Lys) unit as a DNA anchoring moiety was introduced into the amino acid sequence in poly(ethylene glycol)-*b*-cationic poly(*N*-substituted asparagine) with a flanking *N*-(2-aminoethyl)-2-aminoethyl group (PEG-*b*-Asp(DET)) resulting in PEG-*b*-P[Lys/Asp(DET)], in which the Asp(DET) unit acts as a buffering moiety inducing endosomal escape with minimal cytotoxicity. PEG-*b*-P[Lys/Asp(DET)]/DNA polyplexes exhibited a narrow size distribution of ~90 nm without secondary aggregates at the stoichiometric N/P 1, suggesting the formation of PEG-shielded polyplex micelles. The introduction of Lys units into the catiomer sequence facilitated cellular uptake and a 100-fold higher level of gene expression with PEG-*b*-P[Lys/Asp(DET)]/DNA polyplex micelles prepared even at a lowered N/P 2, possibly due to the enhanced association power of the anchoring Lys units.

Keywords: Gene delivery; PEG; Polyplex micelle; Block copolymer; Nonviral

1. Introduction

In recent years, enormous efforts have been devoted to the development of polycation-based gene delivery systems (polyplexes) due to their safety for clinical use, simplicity of preparation, and adaptability to large-scale production [1,2]. In particular, poly(ethylene glycol)-modified (PEGylated) polyplexes (polyplex micelles) formed through the electrostatic interaction between plasmid DNA (pDNA) and PEG-*b*-polycation copolymers (PEG-based block catiomers) are promising for *in vivo* gene therapy applications. The unique core-shell architecture of PEG-based block catiomers when combined with pDNA shows particle size data <100 nm under physiological conditions [3]. Indeed, polyplex micelles from PEG-*b*-poly(L-lysine) copolymers showed a high colloidal stability in biological media, excellent biocompatibility, and prolonged circulation periods in the blood stream [4–6]. However, further improvement in the transfection efficacy of these polyplex systems is needed for translation into the clinic.

Previous studies have revealed that a high transfection efficacy was obtained from polycations with a relatively low p*K*a value, such as polyethylenimine (PEI), which is explained by their buffering effect in endosomal compartments, as described by the proton sponge hypothesis [7,8]. In this regard, we have developed PEG-*b*-poly(*N*-substituted asparagine) copolymers having the *N*-(2-aminoethyl)-2-aminoethyl group

* Corresponding author. Department of Materials Engineering, School of Engineering, The University of Tokyo, 7-3-1 Hongo, Bunkyo-ku, Tokyo 113-8656, Japan. Fax: +81 3 5841 7139.
E-mail address: kataoka@bmw.t.u-tokyo.ac.jp (K. Kataoka).

0168-3659/$ - see front matter © 2007 Elsevier B.V. All rights reserved.
doi:10.1016/j.jconrel.2007.06.020

in the side chain (PEG-*b*-PAsp(DET)). Consequently, these polyplex micelles exhibited a remarkably high transfection activity possibly due to the high buffering capacity based on the distinctive two-step protonation behavior of the flanking ethylenediamine moiety [9]. Also, we found that PEG-*b*-PAsp (DET) copolymers showed minimal cytotoxicity, allowing the successful transfection to primary cells [9–12]. However, an excess of PEG-*b*-PAsp(DET) copolymers with high N/P ratios were required for successful polyplex transfection; consequently, we concluded that micelle solutions prepared under such conditions are likely to contain a mixed population of: (i) block catiomers firmly condensing DNA, (ii) block catiomers loosely associated with DNA, and (iii) free or non-DNA condensing block catiomers. Hence, *in vivo* use of such PEG-*b*-PAsp(DET) polyplex micelles, particularly for systemic administration, may be limited, because loosely associated block catiomers easily desorb from the polyplex micelles during blood circulation, leading to the decreased transfection efficacy at the target site. Therefore, the micelle systems showing efficient transfection at lower N/P ratios without such non-associated or loosely associated catiomers should be next developed for *in vivo* gene delivery.

The present study was devoted to improving the transfection efficacy of the PEG-*b*-PAsp(DET)-based polyplex micelles at N/P ratios near unity by enhancing their association power through the introduction of Lys residues into the amino acid sequence of the block catiomer. Note that Lys residues are expected to anchor the associated block catiomers to the polyplex micelles. In this way, a significantly improved efficacy of transfection was achieved with the polyplex micelles with a subtle excess of block catiomers even after preincubation in the medium containing serum. This result seems to be associated with the facilitated cellular internalization of the polyplex micelles with stably incorporated block catiomers showing a high buffering capacity for endosomal escape.

2. Materials and methods

2.1. Materials

α-Methoxy-ω-amino-poly(ethylene glycol) (Mw 12,000) and β-benzyl-L-aspartate *N*-carboxyanhydride (BLA-NCA) were obtained from Nippon Oil and Fats Co., Ltd. (Tokyo, Japan). ε-(Benzyloxycarbonyl)-L-lysine *N*-carboxyanhydride (Lys(Z)-NCA) was synthesized from ε-(benzyloxycarbonyl)-L-lysine (Wako Pure Chemical Industries, Ltd., Osaka, Japan) by the Fuchs–Farthing method using bis(trichloromethyl) carbonate (triphosgene) (Tokyo Kasei Kogyo Co., Ltd., Tokyo, Japan) [13]. Diethylenetriamine (DET), *N,N*-dimethylformamide (DMF), dichloromethane, benzene, and trifluoroacetic acid were purchased from Wako Pure Chemical Industries, Ltd. Hydrogen bromide (HBr) (30% in acetic acid) was purchased from Tokyo Kasei Kogyo Co., Ltd. Branched polyethylenimine (25 kDa) (BPEI) was purchased from Sigma-Aldrich Co. (St. Louis, MO). The pDNA coding for *luciferase* with a CAG promoter (RIKEN, Japan) was amplified in competent DH5α *E. coli* and purified with a QIAGEN HiSpeed Plasmid MaxiKit (Germantown, MD). Luciferase Assay System Kit was purchased from Promega (Madison WI); Label IT Fluorescein Labeling Kit from Mirus Co. (Milwaukee, WI); and Micro BCA™ Protein Assay Reagent Kit from Pierce Co., Inc. (Rockford, IL).

2.2. Synthesis of PEG-b-P[Lys/Asp(DET)]

Block copolymers of PEG and L-lysine(Z)/β-benzyl-L-aspartate copolymer (P[Lys(Z)/BLA]), further referenced as PEG-*b*-P[Lys(Z)/BLA], were synthesized by ring-opening polymerization of a mixture of Lys(Z)-NCA and BLA-NCA initiated by the terminal primary amino group of α-methoxy-ω-amino-PEG (Scheme 1). The typical synthetic procedure is described as follows for the PEG-*b*-P[Lys(Z)/BLA] with 47 units of Lys(Z) and 52 units of BLA. Lys(Z)-NCA (1.29 g) and BLA-NCA (1.25 g) were dissolved in a mixture of DMF and dichloromethane (6.8 mL and 31.7 mL, respectively). This NCA solution was added to the PEG (1.0 g) in dichloromethane (15 mL) in a stream of dry argon and stirred at 35 °C for 48 h for copolymerization. The polymer in the reaction medium was precipitated in a mixture of hexane and ethyl acetate (600 mL and 400 mL, respectively), and purified by filtration. The acetylation of the *N*-terminal amino group of the obtained polymer (1.5 g) was subsequently performed at 35 °C for 1 h using acetic anhydride (500 μL) in a dichloromethane solution (22 mL). The polymer solution was precipitated into a mixture of hexane and ethyl acetate (300 mL and 200 mL, respectively), purified by filtration, and lyophilized from a benzene solution. The resulting copolymers had molecular weight distributions (Mw/Mn) of 1.1 to 1.3 as determined by GPC (data not shown). The degree of polymerization (DP) of the P[Lys(Z)/BLA] segment in the PEG-*b*-P[Lys(Z)/BLA] was determined from the peak intensity ratio of the methylene protons of PEG (OCH_2-CH_2, δ=3.5 ppm) to the aryl protons of the benzyl groups in the

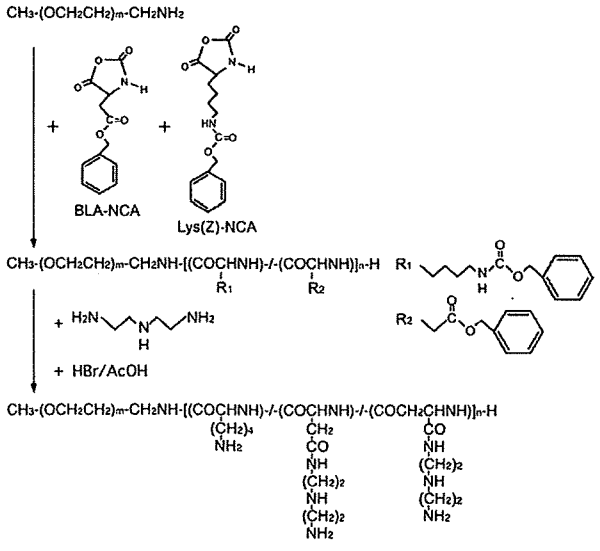

Scheme 1. Synthetic procedure of PEG-*b*-P[Lys/Asp(DET)].

Lys(Z) and BLA units (C_6H_6, δ=7.2–7.3 ppm) in the ^{1}H NMR spectra taken in dimethylsulfoxide at 80 °C. The compositions of the P[Lys(Z)/BLA] segments were determined from the peak intensity ratio of the protons of the β to δ methylene groups ($CH_2CH_2CH_2$, δ=1.2–2.0 ppm) in the side chain of the Lys(Z) units to the protons of the benzyl groups in the Lys(Z) and BLA units in the ^{1}H NMR spectra under the same conditions.

The PEG-*b*-P[Lys(Z)/BLA] copolymers (300 mg) were dissolved in DMF (6 mL), after which DET (2.5 mL; 50 eq to the benzyl group of PBLA) was added to the polymer solution, and stirred for 24 h at 40 °C under a dry argon atmosphere. After 24 h, the mixture was dropped into diethylether (120 mL) with stirring, and then the white precipitate was filtered and re-dissolved in trifluoroacetic acid (4 mL). To deprotect the Z group, HBr (30% in acetic acid) was then added and stirred for 1 h, after which the solution was dropped into diethylether (100 mL) with stirring, and the resulting precipitate was purified by filtered and dried *in vacuo*. The crude product was dissolved in distilled water, dialyzed against 0.01 N HCl and distilled water, and lyophilized to obtain the final product, PEG-*b*-P[Lys/Asp(DET)] as the hydrochloride salt form. The PEG-*b*-P[Lys/Asp(DET)] copolymers with varying ratios of Lys units to Asp (DET) units were obtained by changing the initial feeding ratio of Lys(Z)-NCA to BLA-NCA upon polymerization. The introduction of a DET moiety was confirmed from the peak intensity ratio of the methylene protons of PEG (OCH_2CH_2, δ=3.5 ppm) to the methylene protons of the introduced DET moieties ($CH_2CH_2NHCH_2CH_2$, δ=2.6–3.6 ppm) in the ^{1}H NMR spectra taken in D_2O at 25 °C.

2.3. Preparation of polyplex micelles from PEG-b-P[Lys/Asp (DET)]

The synthesized PEG-*b*-P[Lys/Asp(DET)] copolymer was dissolved in 10 mM Tris–HCl (pH 7.4) buffer at 5 mg/mL. This polymer solution was then mixed with pDNA in 10 mM Tris–HCl (pH 7.4) (50 μg/mL) at varying N/P ratios (residual molar ratio of amino groups in Lys and Asp(DET) units to pDNA phosphate groups), followed by a 24 h incubation at ambient temperature. The final concentration of pDNA in all the samples was adjusted to 33 μg/mL. The complexation of pDNA with the polycations was confirmed by agarose gel retardation analysis and ethidium bromide (EtBr) dye exclusion assay. In the gel retardation analysis, each sample was prepared by the dilution of the micelle solutions to the concentration of 8.3 μg pDNA/mL. 20 μL of each sample (166 ng pDNA) with a loading buffer was then electrophoresed at 100 V for 1 h on a 0.9 wt% agarose gel in 3.3 mM Tris–acetic acid buffer containing 1.7 mM sodium acetate. The migrated pDNA was visualized by soaking the gel in distilled water containing EtBr (0.5 μg/mL). In the EtBr dye exclusion assay, each sample (33 μg pDNA/mL) with varying N/P ratios was adjusted to 10 μg pDNA/mL with 2.5 μg EtBr/mL and 150 mM NaCl by adding 10 mM Tris–HCl (pH 7.4) buffer containing EtBr and NaCl. The solutions were incubated at ambient temperature overnight. The fluorescence intensity of the samples excited at 510 nm was measured at 590 nm and a temperature of 25 °C using a spectrofluorometer (Jasco, FP-777). The relative fluorescence intensity was calculated as follows:

$$F_r = (F_{sample} - F_0)/(F_{100} - F_0)$$

where F_{sample} is the fluorescence intensity of the micelle samples, F_{100} is the free pDNA, and F_0 is the background without pDNA.

2.4. Zeta-potential and dynamic light scattering (DLS) measurements

The zeta-potential of the polyplex micelles was determined from the laser-Doppler electrophoresis using the Zetasizer nanoseries (Malvern Instruments Ltd., UK) at a detection angle of 173° and a temperature of 25 °C. Each sample was prepared by simply mixing the polymer solutions with the pDNA solution at varying N^+/P ratios (33 μg pDNA/mL). The N^+/P ratio was defined as the residual molar ratio of protonated amino groups in PEG-*b*-P[Lys/Asp(DET)] to phosphate groups in DNA. The fraction of protonated amino groups in P[Lys/Asp(DET)] segment was calculated assuming that 100% and 50% of the amino groups in the Lys and Asp(DET) units, respectively, were protonated at pH 7.4 and a temperature of 25 °C based on the potentiometric titration results [9]. The samples were adjusted to 14 μg pDNA/mL by adding 10 mM Tris–HCl (pH 7.4) buffer, and then, injected into folded capillary cells (Malvern Instruments, Ltd.), followed by the measurement. From the obtained electrophoretic mobility, the zeta-potentials of each micelle were calculated by the Smoluchowski equation: $\zeta = 4\pi\eta\upsilon/e$ in which η is the viscosity of the solvent, υ is the electrophoretic mobility, and e is the dielectric constant of the solvent. The results are represented as the average of three experiments.

The sizes of each polyplex micelle were also measured by the DLS using the same apparatus. Micelle samples were prepared by mixing each polymer solution with pDNA solution at varying N^+/P ratios (33 μg pDNA/mL). After an overnight incubation at ambient temperature, the samples were adjusted to 14 μg pDNA/mL by adding 10 mM Tris–HCl (pH 7.4) buffer, and then injected into low volume glass cuvettes, ZEN2112 (Malvern Instruments, Ltd.), followed by the measurement. The data obtained from the rate of decay in the photon correlation function were analyzed by the cumulant method, and the corresponding hydrodynamic diameter of micelles was then calculated by the Stokes–Einstein equation [14].

2.5. Stability of polyplex micelles against counter polyanion exchange reaction

The stability of the polyplex micelle was estimated from the release of pDNA from the micelle caused by the exchange reaction with poly(aspartic acid) (PAsp, DP 66) as a polyanion. Ten mM Tris–HCl buffer (pH 7.4) solutions with varying concentrations of PAsp were added to the micelle solution with the pDNA concentration of 33 μg/mL. After overnight incubation at ambient temperature, each sample solution containing 167 ng of pDNA was electrophoresed through a 0.9 wt% agarose gel with

a running buffer of (3.3 mM Tris–acetic acid (pH 7.4)+1.7 mM sodium acetate+1 mM EDTA2Na). The pDNAs in the gel were visualized by soaking the gel into distilled water containing EtBr (0.5 mg/L).

2.6. Radiolabeling of pDNA for the cellular uptake study of polyplex micelles

pDNA was radioactively labeled with ^{32}P-dCTP using the Nick Translation System (Invitrogen, San Diego, CA). Unincorporated nucleotides were removed using High Pure PCR Product Purification Kit (Roche Laboratories, Nutley, NJ). After the purification, the 2 μg of labeled pDNA was mixed with 400 μg of non-labeled pDNA. The polyplex micelle samples were prepared by mixing the radioactive pDNA solution with each polymer solution (33 μg pDNA/mL). For cellular uptake experiments, Hela cells were seeded on 24-well cultured plates 24 h before the experiments in Dulbecco's modified Eagle medium (DMEM) containing 10% fetal bovine serum (FBS). The cells were incubated with 30 μL of the radioactive micelle solution (1 μg pDNA/well) in 400 μL of DMEM containing 10% FBS. After 24 h incubation, the cells were washed three times with Dulbecco's PBS and lysed with 400 μL of the cell culture Promega lysis buffer. The lysates were mixed with 5 mL of scintillation cocktail, Ultima Gold (PerkinElmer, MA), and then, the radioactivity of the lysate solution was measured by a scintillation counter. The results are presented as a mean and standard error of mean obtained from four samples.

2.7. In vitro transfection

Hela cells were seeded on 24-well culture plates and incubated overnight in 400 μL of DMEM containing 10% FBS. The medium was changed to 400 μL of fresh DMEM containing 10% FBS, and then 30 μL of each micelle solution was applied to each well (1 μg of pDNA/well). In the estimation of the effect of serum incubation on the transfection capacity of the micelle samples, the micelle solutions were preincubated with DMEM containing 10% FBS for 4 h and then added to the wells. After 24 h incubation, the medium was changed to 400 μL of fresh DMEM without micelle samples, followed by an additional 24 h incubation. The cells were washed with 400 μL of Dulbecco's PBS, and lysed by 100 μL of the cell culture Promega lysis buffer. The luciferase activity of the lysates was evaluated from the photoluminescence intensity using Mithras LB 940 (Berthold Technologies). The obtained luciferase activity was normalized with the amount of proteins in the lysates determined by the Micro BCA™ Protein Assay Reagent Kit (Pierce).

Table 1
A series of synthesized block catiomers

Code	Feeding unit radio (Lys: Asp)	DP of poly (amino acid)	Unit number of Lys in poly(amino acid)	% of Lys units
L0/101	0:120	101	0	0
L24/102	25:90	102	24	24
L47/99	50:60	99	47	47
L70/98	75:30	98	70	71
L109/109	120:0	109	109	100

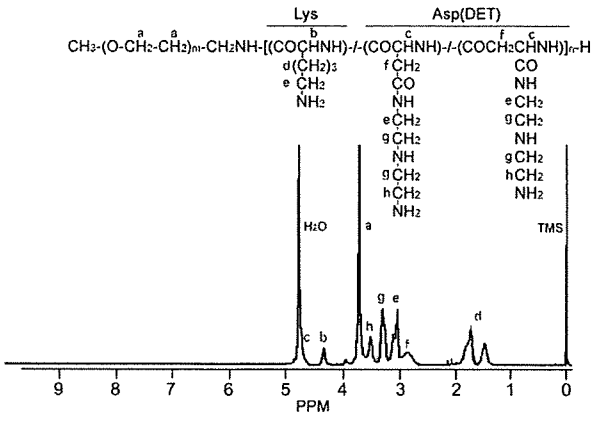

Fig. 1. ^{1}H-NMR spectrum of the PEG-*b*-P[Lys/Asp(DET)] (L47/99) (D_2O; 25 °C; concentration, 10 mg/mL).

2.8. Tolerability of polyplex micelles in serum-containing medium

The tolerability of polyplex micelles in serum-containing medium was estimated from the change in the fluorescence intensity of the fluorescein-labeled pDNA (F-pDNA) contained in the micelles. A pDNA was labeled using a Label IT Fluorescein Labeling Kit. This system promotes the covalent attachment of specific fluorescent molecules to guanine residues in nucleic acids. Each polyplex micelle sample was prepared by simply adding the polymer solution to the F-pDNA solution. After an overnight incubation at ambient temperature under dark conditions, the micelle solutions were mixed with 9 times volume of FBS solution, and then incubated at 37 °C for 4 h. The fluorescence emission of each sample excited at 492 nm was measured at 520 nm and a temperature of 37 °C using a spectrofluorometer (Jasco, FP-777). The obtained fluorescence intensities were expressed as the relative value to the fluorescence intensity of naked F-pDNA.

3. Results and discussion

3.1. Synthesis of PEG-b-P[Lys/Asp(DET)]

Block copolymers of PEG and P[Lys(Z)/BLA] (PEG-*b*-P[Lys(Z)/BLA]) were prepared by the ring-opening copolymerization of Lys(Z)- and BLA-NCAs as shown in Scheme 1. The poly(amino acid) segments with similar DP and varying Lys(Z)/BLA unit ratios were synthesized by changing the feeding ratio of Lys(Z)-NCA to BLA-NCA in the reaction mixture. The DPs and the unit ratios of Lys(Z)/BLA in the obtained copolymers were calculated from the peak intensity ratio in the ^{1}H NMR spectra (data not shown). As summarized in Table 1, five types of copolymers were prepared. The DP of the poly(amino acid) segments in a series of copolymers was confirmed to be approximately 100, regardless of the composition. These copolymers were then subjected to aminolysis reaction with DET, followed

by deprotection of the Z groups. The ^{1}H NMR spectra of the obtained catiomers, as typically seen in Fig. 1, reveal the quantitative aminolysis of BLA units as well as the complete deprotection of Lys(Z) units in the poly(amino acid) segment, because the methylene protons in the DET moiety and the β-methylene protons in the asparagine unit had a 4:1 peak intensity ratio and the peaks of the Z group disappeared in the ^{1}H NMR spectrum. These catiomers were abbreviated as L*x*/*y*, where *x* and *y* represent the unit number of Lys and the total DP of the poly(amino acid) segment, respectively.

3.2. Formation of polyplex micelles from PEG-b-P[Lys/Asp (DET)] catiomers

The polyplex micelles were prepared by simply mixing each catiomer solution with pDNA solution at varying N/P ratios. The complex formation of pDNA was confirmed by the agarose gel electrophoresis of each sample. With an increase in the N/P ratio, the amount of migrating free pDNA decreased, indicating the complex formation of pDNA with the PEG-*b*-P[Lys/Asp (DET)] catiomers (Supplementary Fig. 1). The critical N/P ratio where the migration of pDNA was completely retarded differed depending on the composition of the catiomers; i.e., the micelle of the block catiomers with a lower ratio of Lys units required the higher N/P ratio for the complete retardation of pDNA. To quantitatively evaluate the relationship between the N/P ratio and the condensation behavior of pDNA, the EtBr dye exclusion assay by fluorometry was completed. Fig. 2 (a) shows that the fluorescence intensity of EtBr decreased with an increase in the N/P ratio, and leveled off at a critical N/P ratio for each micelle system. These fluorescence data were then replotted against N^+/P ratio, the molar ratio of protonated amino groups at pH 7.4 in the block catiomers to phosphate groups in pDNA, as seen in Fig. 2 (b). Note that the ratios of the protonated amino groups in the block catiomer were calculated as 100% for Lys units and 50% for Asp(DET) units at pH 7.4, respectively, from the potentiometric titration results of PEG-*b*-PLys and PEG-*b*-PAsp(DET) block catiomers [9,15]. Interestingly, Fig. 2 (b) reveals that the fluorescence intensity of all the micelles leveled off at the N^+/P ratio of approximately 1 regardless of the composition of the catiomers, indicating that the condensation behavior of pDNA might be closely correlated with the ratio of charged groups (N^+/P). Also, this result strongly suggests that the PAsp(DET) segment in the micelles is likely to maintain the same protonation degree (α=0.5 at pH 7.4) as that in the free catiomer without the facilitated protonation by the complexation. As previously reported [9], this limited protonation for the proton sponge potential of the Asp(DET) units in the micelles is assumed to contribute to endosomal escape of PEG-*b*-P[Lys/Asp(DET)] polyplex micelles.

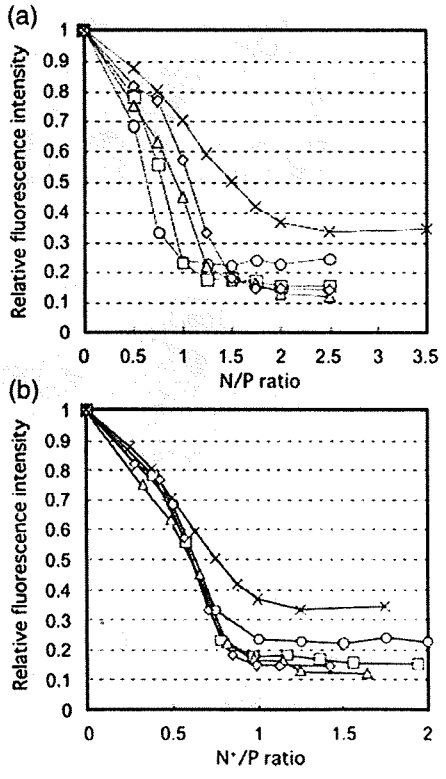

Fig. 2. EtBr dye exclusion assay on a series of polyplex micelles. Micelles included are: ×: L0/101; ◇: L24/102; △: L47/99; □: L70/98; ○: L109/109. (a) Relative fluorescence intensity vs. N/P ratio. (b) Relative fluorescence intensity vs. N^+/P ratio.

Fig. 3 (a) and (b) show the results obtained from DLS and zeta-potential measurements. The cumulant diameters of the polyplex micelles from the PEG-*b*-P[Lys/Asp(DET)]s were determined to be 70–100 nm throughout the range of the examined N^+/P > 1. As seen in the Fig. 3 (b) inset, the zeta-potentials of each polyplex micelle appear nearly neutral at an N^+/P 1, indicating the formation of the charge stoichiometric micelle from pDNA and the block catiomers. It should be emphasized that the polyplex micelles from PEG-*b*-P[Lys/Asp(DET)] had a narrowly distributed size of approximately 90 nm without secondary aggregates even at the charge neutralized condition (N^+/P 1) as previously demonstrated for those from PEG-*b*-PLys and PEG-*b*-PAsp(DET) catiomers [9,16]. It should also be noted that all polyplex micelles from the block catiomers had a much lower absolute value in zeta-potentials than polyplexes prepared from PAsp(DET) homopolymer (DP 98) (Fig. 3 (b)), possibly due to the shielding effect of the PEG layer surrounding the polyplex core. Nevertheless, there was a slight increase in the zeta-potentials of the polyplex micelles from neutral to positive values in the region of N^+/P > 1. This zeta-potential increase is likely to be ascribed to the loose association of excess catiomers with the polyplex micelles as previously reported for the PEG-poly(2-dimethylamino)ethyl methacrylate) catiomer/pDNA micelle [17]. Interestingly, the tendency of such increasing zeta-potentials with N^+/P ratios varied according to the composition of the block catiomers. The zeta-potential value of the polyplex micelles from PEG-*b*-PLys leveled off at an N^+/P 4 (+10 mV), while that from PEG-*b*-PAsp(DET) seemed to reach a plateau at a higher N^+/P 16 (+10 mV), suggesting that the association profile of the block catiomers with the polyplex micelles varied between PEG-*b*-PLys and PEG-*b*-PAsp(DET) micelles at N^+/P ratios ranging from 1 to 16. Presumably, PEG-*b*-PLys may reach the saturated association with pDNA at the lower

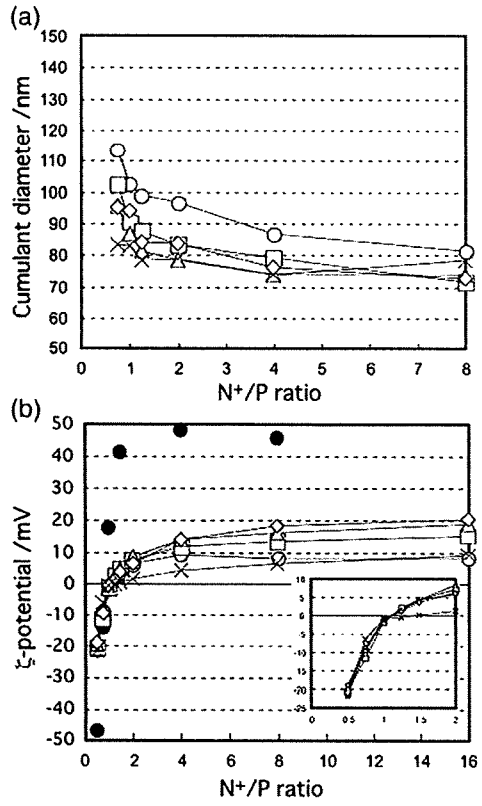

Fig. 3. (a) Size and (b) ζ-potential of a series of polyplex micelles and a PAsp (DET) polyplex. ×: L0/101 micelle, ◇: L24/102 micelle, △: L47/99 micelle, □: L70/98 micelle, ○: L109/109 micelle, ●: PAsp(DET) (DP 98) polyplex.

concentration (lower N^+/P) than PEG-*b*-PAsp(DET) due to the effective anchoring effect of the Lys units. Although PEG-*b*-P[Lys/Asp(DET)] micelles displayed the similar profiles of the zeta-potential to PEG-*b*-PLys micelles at lower N^+/P ratios, the micelles showed further increase in the surface charge in the range of $N^+/P>4$ without leveling off. This result suggests that the association of PEG-*b*-P[Lys/Asp(DET)] with pDNA may not be saturated even in the range of $N^+/P>4$, despite introduction of Lys units as a DNA anchoring moiety. This phenomenon may be ascribed to the unique structure of PEG-*b*-P[Lys/Asp(DET)] possessing two types of cationic units with different pDNA affinity. The presence of the Lys units in the block catiomer is likely to facilitate the binding of Asp (DET) units to pDNA, promoting the block catiomer association to the polyplex micelles at N^+/P 2 or lower; however, at high concentrations of the block catiomers (high N^+/P), Lys units may preferentially bind to the polyplex micelles to replace the Asp (DET) units, resulting in the continuous binding of the block catiomers until the Lys units saturate the available binding sites.

3.3. Stability of polyplex micelles

The result of the zeta-potential measurement suggested that the affinity of PAsp(DET) to pDNA seems to be enhanced by the incorporation of Lys units. The complexing stability of the polyplex micelles prepared from PEG-*b*-P[Lys/Asp(DET)] was evaluated directly from the standpoint of the counter polyion exchange reaction. The solutions with varying concentrations of PAsp were added to the solution of the PEG-*b*-PAsp(DET) micelle (N^+/P 2) in different A/P ratios (the molar ratio of carboxyl groups of PAsp to phosphate groups of pDNA). Consequently, the pDNA was released from the PEG-*b*-PAsp (DET) micelles at A/P>3 due to the counter polyanion exchange of pDNA by PAsp (Fig. 4 (a)). In contrast, the improved stability of the polyplex micelles from PEG-*b*-P[Lys/Asp(DET)] was

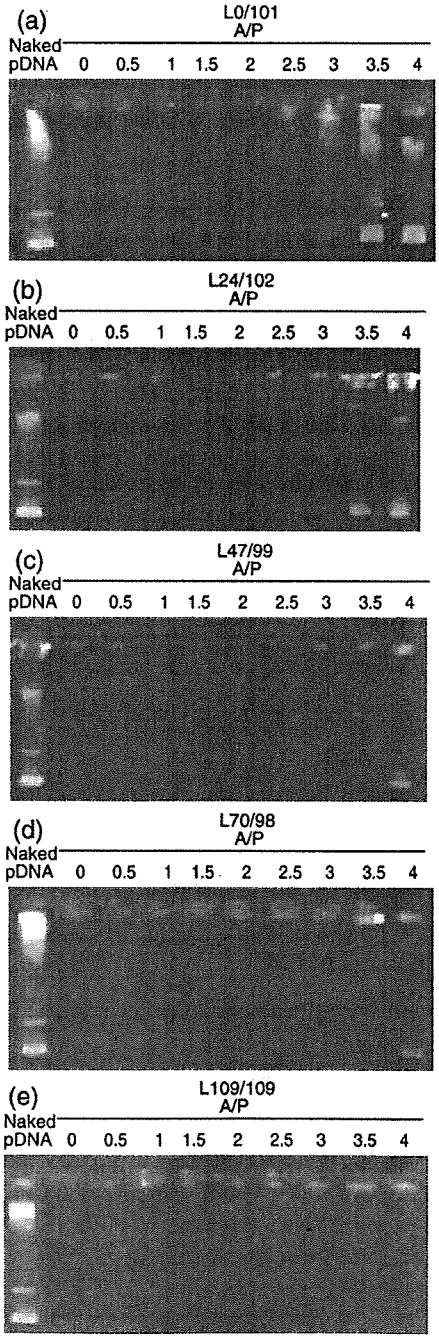

Fig. 4. Electrophoretic evaluation of polyplex micelle (N^+/P 2) tolerability against an exchange reaction with polyaspartic acid (DP 66). Note: A/P stands for the molar ratio of carboxyl groups in polyaspartic acid to phosphate groups in pDNA. Micelle samples prepared at N^+/P 2 were mixed with polyaspartic acid solution and electrophoresed after overnight incubation.

confirmed as shown in Fig. 4 (b)–(d): higher A/P ratios were required for the pDNA release with the increment in the percentage of Lys units in the amino acid sequence of the PEG-*b*-P[Lys/Asp(DET)]. In the case of the micelles from PEG-*b*-PLys, the pDNA release was not observed in the range of the examined A/P ratios (0–4) (Fig. 4 (e)). The similar tendency was also confirmed for the micelles prepared at N^+/P 4 (Supplementary Fig. 2). These results support our hypothesis that a Lys unit has a higher association power with pDNA than the Asp(DET) unit, and consequently, the PEG-*b*-P[Lys/Asp(DET)] micelles acquired the tolerability against the dissociation by polyanions through the anchoring effect of Lys units in the block catiomer.

3.4. Transfection with polyplex micelles from PEG-b-P[Lys/Asp(DET)]

Preliminary experiments on the cellular uptake of complexed pDNA revealed that the pDNA incorporated into PEG-*b*-PAsp (DET) at $N^+/P<4$ was marginally internalized by cultured cells as is the case with naked pDNA (Supplementary Fig. 3). We speculate that this may contribute to the significantly lower transfection ability of PEG-*b*-PAsp(DET) micelles prepared at low N^+/P ratios. Herein, we hypothesize that the complexing stability promoted by the Lys anchors may facilitate the cellular uptake of polyplex micelles prepared even at low N^+/P ratios. To confirm this hypothesis, we completed a cellular uptake study using ^{32}P-radiolabeled pDNA. Fig. 5 reveals that the cellular uptake of pDNA complexed with block catiomers at an N^+/P ratio of 2 increased by the introduction of the Lys unit into the amino acid sequence. Especially, the polyplex micelles from the PEG-*b*-P[Lys/Asp(DET)] with the percentage of Lys units >47 exhibited more than a 10-fold uptake of pDNA compared to PEG-*b*-PAsp (DET). This result strongly suggests that the increased association power of the polyplex micelles may contribute to their facilitated cellular uptake without a large excess of block catiomers, i.e., at low N^+/P ratios. Interestingly, the cellular uptake of radioactive pDNA was maximized at the L70/98, even through its stability was deemed comparable to that of PEG-*b*-PLys (L109/109), as evidenced from the counter polyanion exchange reaction (Fig. 4

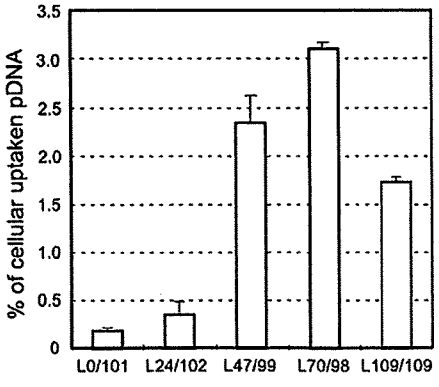

Fig. 5. The uptake of pDNA complexed with block catiomers at N^+/P 2 into Hela cells. ^{32}P-labeled pDNA micelles were incubated with the cells in DMEM containing 10% FBS at 37 °C for 24 h. The amount of internalized pDNA is represented as a percentage for the dosed pDNA (1 μg/well).

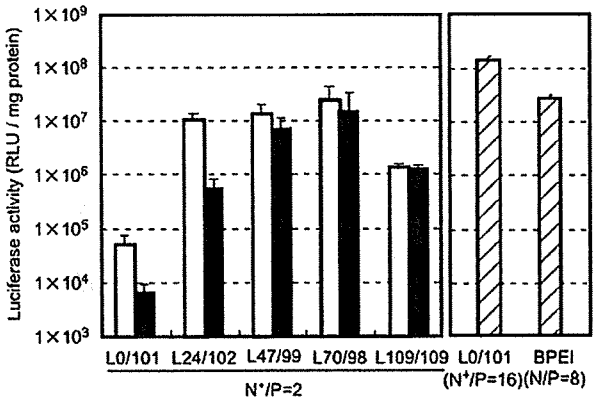

Fig. 6. *In vitro* transfection efficacy of polyplex micelles (N^+/P 2) against Hela cells. Open bars: Transfection efficacy without serum-preincubation. Closed bars: Transfection efficacy after 4 h incubation in the DMEM containing 10% FBS. Hatched bars: Transfection efficacy of the control; L0/101 micelles (N^+/P 16) and BPEI (25 kDa) polyplexes (N/P 8).

(d) and (e)). These data indicate that the increased cellular uptake of PEG-*b*-P[Lys/Asp(DET)] micelles compared to PEG-*b*-PLys micelles was not simply correlated to the enhanced stability. In this regard, a slightly positive zeta-potential of PEG-*b*-P[Lys/Asp (DET)] micelles compared to PEG-*b*-PAsp(DET) and PEG-*b*-PLys micelles is noteworthy, suggesting the surface charge may indeed affect the cellular uptake of the micelles with varying stabilities.

The effect of the introduction of the Lys unit as an anchoring moiety on the transfection ability of the polyplex micelles was then evaluated from the expression of a luciferase gene in the transfected cells. Although the PEG-*b*-PAsp(DET) micelles prepared at the high N^+/P 16 (ca. N/P 32) showed appreciably high transfection efficacy, which was one order of magnitude higher than that of BPEI polyplexes (25 kDa, N/P 8), reduction in the N^+/P ratio resulted in a sharp decline of the transfection ability of the PEG-*b*-PAsp(DET) micelles probably due to the lowered cellular uptake (Fig. 6). In contrast, the transfection efficacy could be maintained to be a high value even in the range of lowered N^+/P ratios by introducing Lys units into the block catiomer (Supplementary Fig. 4). Eventually, the PEG-*b*-P[Lys/Asp(DET)] micelles revealed an appreciably improved transfection efficacy at N^+/P 2 compared to the polyplex micelles of PEG-*b*-PLys and PEG-*b*-PAsp(DET) (Fig. 6, open bars). These results suggest that PEG-*b*-P[Lys/Asp(DET)] micelles may provide high stability and promote endosomal escape, presumably due to the synergistic effect of Lys and Asp(DET) units. The improved stability through the anchoring effect of Lys units was also confirmed from the transfection results after the preincubation of micelles in the serum-containing medium (Fig. 6, closed bars). The micelles from PEG-*b*-P[Lys/Asp(DET)], with the higher percentage of Lys units (L47/99 and L70/98), maintained the initial transfection capacity even after the serum-preincubation, whereas transfection efficacies of PEG-*b*-PAsp(DET) and L24/102 micelles, with a low percentage of Lys residues, were significantly impaired by serum-preincubation. These results strongly suggest that the associated block catiomers in the micelles from L47/99, L70/98, and L109/109 might be tolerable

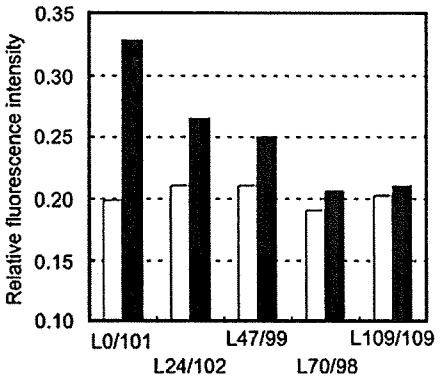

Fig. 7. Tolerability of polyplex micelles against serum incubation evaluated from the fluorescence recovery of the entrapped fluorescein-labeled pDNA due to serum-induced decondensation. Open bars: Fluorescence intensity in 10 mM Tris–HCl (pH 7.4) buffer solution without FBS. Closed bars: Fluorescence intensity after 4 h incubation in the medium containing 90% FBS.

in the transfection medium containing serum due to the strong anchoring of Lys units. This added strength of the Lys anchors is further supported by the sustained fluorescence quenching of fluorescein-labeled pDNA in micelles incubated in 90% FBS for 4 h as seen in Fig. 7. Apparently, fluorescence recovery due to the serum-inducing decondensation of pDNA was progressively inhibited with the increment in the percentage of Lys units in the PEG-*b*-P[Lys/Asp(DET)].

Although the transfection efficacy (Fig. 6) seems to be roughly correlated with the cellular uptake of the micelles (Fig. 5), careful examination reveals the tendency that the PEG-*b*-P[Lys/Asp(DET)] micelles with the lower percentage of Lys units, L24/102, achieved comparable transfection to those with the higher percentage of Lys units, 47/L98 and L70/98, even though the efficacy of pDNA uptake was fairly limited. This tendency becomes more apparent by normalizing the luciferase activity with pDNA uptake (Supplementary Fig. 5). This apparent increase in the transfection efficacy may be explained by the timely release of the loosely associated block catiomers from the micelles in the endosomal compartment to exert a high buffering capacity [9] and their possible interaction with the endosomal membrane component, facilitating the endosomal escape of the complexed pDNA, followed by a smooth release of pDNA directing efficient transcription. The loosely associated nature of L24/102 in the micelle may be supported from a decreased transfection efficacy after serum-preincubation as shown in Fig. 6.

4. Conclusion

Polyplex micelles from PEG-*b*-PAsp(DET) revealed a high transfection efficacy to various cell types including primary cells [9–12] presumably due to a low cytotoxicity and a strong pH-buffering capacity. Nevertheless, the weak association power of PAsp(DET) with DNA may be problematic for *in vivo* systemic administration, where the tolerability of polyplexes in proteinaceous media should be a crucial factor. Alternatively, a polylysine has an appreciably high affinity to DNA, however, the transfection efficacy of polylysine polyplexes remains low, possibly due to poor endosomal escaping functions and an impaired release of pDNA from the polyplex with an over-stabilized nature. In this novel study, we sought to alter these discrepancies by placing both Asp(DET) as a buffering unit with low cytotoxicity and Lys as a strong anchoring moiety to DNA in a single polymer strand resulting in PEG-*b*-P[Lys/Asp(DET)]. Polyplexes prepared from pDNA and PEG-*b*-P[Lys/Asp(DET)] have a micellar structure with a PEG palisade, exhibiting a remarkably improved stability compared to PEG-*b*-PAsp(DET)/pDNA polyplex micelles. PEG-*b*-P[Lys/Asp(DET)] polyplex micelles were further revealed to promote cellular internalization, leading to enhanced transfection efficacy even with a subtle excess of block catiomers. This enhanced transfection efficacy could be explained by the synergistic effect of Lys as an anchoring unit and Asp(DET) as a lower toxic endosomal escaping unit. This approach of placing cationic units with discriminating functions, e.g., DNA anchoring and endosomal escaping functions, into a single block catiomer strand is highly promising for future construct designs for effective *in vivo* systemic applications.

Acknowledgement

This work was financially supported by Research Fellowships of the Japan Society for the Promotion of Science for Young Scientists (JSPS), the Mitsubishi Chemical Corporation Fund, and the Core Research Program for Evolutional Science and Technology (CREST) from the Japan Science and Technology Corporation (JST). The authors express their appreciation to Dr H. Hamada (RIKEN, Japan) for providing the plasmid DNA.

Appendix A. Supplementary data

Supplementary data associated with this article can be found, in the online version, at doi:10.1016/j.jconrel.2007.06.020.

References

[1] D.W. Pack, A.S. Hoffman, S. Pun, P.S. Stayton, Design and development of polymers for gene delivery, Nat. Rev. Drug Discov. 4 (2005) 581–593.
[2] E. Mastrobattista, M.A.E.M. van der Aa, W.E. Hennink, D.J.A. Crommelin, Artificial viruses: a nanotechnological approach to gene delivery, Nat. Rev. Drug Discov. 5 (2006) 115–121.
[3] K. Kakizawa, K. Kataoka, Block copolymer micelles for delivery of gene and related compounds, Adv. Drug Deliv. Rev. 54 (2002) 203–222.
[4] K. Itaka, A. Harada, K. Nakamura, H. Kawaguchi, K. Kataoka, Evaluation by fluorescence resonance energy transfer of the stability of nonviral gene delivery vectors under physiological conditions, Biomacromolecules 3 (2002) 841–845.
[5] M. Harada-Shiba, K. Yamauchi, A. Harada, I. Takamisawa, K. Shimokado, K. Kataoka, Polyion complex micelles as a vector in gene therapy-pharmacokinetics and in vivo gene transfer, Gene Ther. 9 (2002) 407–414.
[6] K. Miyata, Y. Kakizawa, N. Nishiyama, Y. Yamasaki, T. Watanabe, M. Kohara, K. Kataoka, Freeze-dried formulations for in vivo gene delivery of PEGylated polyplex micelles with disulfide crosslinked cores to the liver, J. Control. Release 109 (2005) 15–23.
[7] O. Boussif, F. Lezoualc'h, M.A. Zanta, M.D. Mergny, D. Scherman, B. Demeneix, J.-P. Behr, A versatile vector for gene and oligonucleotide transfer into cells in culture and in vivo: Polyethylenimine, Proc. Natl. Acad. Sci. U. S. A. 92 (1995) 7297–7301.

[8] M. Neu, D. Fischer, T. Kissel, Recent advances in rational gene transfer vector design based on poly(ethylene imine) and its derivatives, J. Gene Med. 7 (2005) 992–1009.
[9] N. Kanayama, S. Fukushima, N. Nishiyama, K. Itaka, W.-D. Jang, K. Miyata, Y. Yamasaki, K. Kataoka, PEG-based biocompatible block cationer with high-buffering capacity for the construction of polyplex micelles showing efficient gene transfer toward primary cells, ChemMedChem 1 (2006) 439–444.
[10] D. Akagi, M. Oba, H. Koyama, N. Nishiyama, S. Fukushima, T. Miyata, H. Nagawa, K. Kataoka, Biocompatible micellar nanovectors achieve efficient gene transfer to vascular lesions without cytotoxicity and thrombus formation, Gene Ther. 14 (2007) 1029–1038.
[11] M. Han, Y. Bae, N. Nishiyama, K. Miyata, M. Oba, K. Kataoka, Transfection study using multicellular tumor spheroids for screening non-viral polymeric gene vectors with low cytotoxicity and high transfection efficiencies, J. Control. Release, in press.
[12] K. Itaka, S. Ohba, K. Miyata, H. Kawaguchi, K. Nakamura, T. Takato, U. Chung, K. Kataoka, Bone regeneration by regulated in vivo gene transfer using biocompatible polyplex nanomicelles, Mol. Ther., in press.
[13] W.H. Daly, D. Poche, The preparation of *N*-carboxyanhydrides of alpha-amino-acids using bis(trichloromethyl)carbonate, Tetrahedron Lett. 29 (1988) 5859–5862.
[14] A. Harada, K. Kataoka, Formation of polyion complex micelles in an aqueous milieu from a pair of oppositely-charged block-copolymers with poly(ethylene glycol) segments, Macromolecules 28 (1995) 5294–5299.
[15] A. Harada, S. Cammas, K. Kataoka, Stabilized α-helix structure of poly (L-lysine)-block-poly(ethylene glycol) in aqueous medium through supramolecular assembly, Macromolecules 29 (1996) 6183–6188.
[16] K. Itaka, K. Yamauchi, A. Harada, K. Nakamura, H. Kawaguchi, K. Kataoka, Polyion complex micelles from plasmid DNA and poly(ethylene glycol)-poly(L-lysine) block copolymer as serum-tolerable polyplex system: physicochemical properties of micelles relevant to gene transfection efficiency, Biomaterials 24 (2003) 4495–4506.
[17] D. Wakebayashi, N. Nishiyama, K. Itaka, K. Miyata, Y. Yamasaki, A. Harada, H. Koyama, Y. Nagasaki, K. Kataoka, Polyion complex micelles of pDNA with acetal-poly(ethylene glycol)-poly(2-(dimethylamino(ethyl methacrylate) block copolymer as the gene carrier system: Physicochemical properties of micelles relevant to gene transfection efficacy, Biomacromolecules 5 (2004) 2128–2136.